IMPROVED EMPIRICAL WAVELET TRANSFORM FOR NON-STATIONARY SIGNAL ANALYSIS USING FOURIER-BESSEL SERIES EXPANSION

M.Tech Thesis

By

LOKESH SINGH

DISCIPLINE OF ELECTRICAL ENGINEERING
INDIAN INSTITUTE OF TECHNOLOGY INDORE

JULY 2018

IMPROVED EMPIRICAL WAVELET TRANSFORM FOR NON-STATIONARY SIGNAL ANALYSIS USING FOURIER-BESSEL SERIES EXPANSION

A THESIS

Submitted in partial fulfillment of the

requirements for the award of the degree

of

Master of Technology

with specialization in

Communication and Signal Processing

by

LOKESH SINGH

DISCIPLINE OF ELECTRICAL ENGINEERING
INDIAN INSTITUTE OF TECHNOLOGY INDORE

JULY 2018

INDIAN INSTITUTE OF TECHNOLOGY INDORE

CANDIDATE'S DECLARATION

I hereby certify that the work which is being presented in the thesis entitled "**IMPROVED EMPIRICAL WAVELET TRANSFORM FOR NON STATIONARY SIGNAL ANALYSIS USING FOURIER-BESSEL SERIES EXPANSION**" in the partial fulfillment of the requirements for the award of the degree of Master of Technology and submitted in the DISCIPLINE OF ELECTRICAL ENGINEERING, Indian Institute of Technology Indore, is an authentic record of my own work carried out during the time period from July 2017 to July 2018 under the supervision of Prof. Ram Bilas Pachori, Indian Institute of Technology Indore, India.

The matter presented in this thesis has not been submitted by me for the award of any other degree of this or any other institute.

Signature of the student with date

(LOKESH SINGH)

This is to certify that the above statement made by the candidate is correct to the best of my knowledge.

Signature of Thesis Supervisor with date

(Prof. RAM BILAS PACHORI)

Lokesh singh has successfully given his M.Tech Oral Examination held on

Signature of Thesis Supervisor
Date:

Convener, DPGC
Date:

Signature of PSPC Member:1
Date:

Signature of PSPC Member:2
Date:

ACKNOWLEDGEMENTS

Completion of this masters dissertation was possible with the support of several people. I would like to express my sincere gratitude to all of them. I would like to thank my supervisor, Prof. Ram Bilas Pachori, for the patient guidance, encouragement, and advice he has provided throughout my time as his student. I have been extremely lucky to have a supervisor who cared so much about my work, and who responded to my questions and queries so promptly. I could not have imagined having a better advisor and mentor for my M.Tech study. You have been a tremendous mentor for me Sir was always supportive to me whenever I felt low and made himself available to clarify my doubts even in his busy schedule.

Besides my advisor, I would like to thank the PSPC members: Dr. Vivek Kanhangad and Dr. Ritunesh Kumar for their encouragement and insightful comments. I would like to thank Abhijit Bhattacharyya for technical discussions and encouragement, without his continuous cooperation it would have been difficult for me to finish research work within stipulated time. I would like to thank my parents, whose love and guidance are with me in whatever I pursue. also thank my friends for providing support and friendship that I needed. I thank all the present members of the Signal Analysis Research Lab.

LOKESH SINGH

Dedicated
to
My Family

Abstract

This dissertation presents an improved empirical wavelet transform (EWT) for the time-frequency (TF) representation of non-stationary signals. Though the EWT method has been shown its effectiveness in some applications, it becomes difficult to analyze some non-stationary signals due to its improper segmentation in the frequency domain. Spectral analysis using the Fourier transform is a powerful technique for stationary time series where the characteristics of the signal do not change with time. For non-stationary time series like modulated signals, the spectral content changes with time and hence time-averaged amplitude spectrum may be found using Fourier transform. There are serval TF domain based methods available for analysis of non-stationary signals namely short-time Fourier transform (STFT), wavelet transform(WT), Wigner-Ville distribution (WVD), and Hilbert-Huang transform (HHT). The features can be extracted in TF domain for the classification of non-stationary signals. There are other methods namely, tunable-Q wavelet transform (TWQT), empirical mode decomposition (EMD), and variational mode decomposition (VMD). The conventional wavelet based method rely on pre-fixed basis functions to analyze the signals, hence are considered to be rigid or non-adaptive. However, the non-adaptive methods find difficulty in analyzing physical signals due to the existence of closely spaced frequency components.

In this dissertation existing EWT has been enhanced using Fourier-Bessel series expansion (FBSE) in order to obtain improved TF representation of non-stationary signals. The FBSE uses Bessel functions as bases, which are non-stationary in nature. This makes FBSE suitable for analysis of signal with time-varying parameters. There are certain advantages of the FBSE spectrum representation. It has been observed that FBSE spectrum has compact representation as compared to conventional Fourier representation. Secondly, FBSE spectrum avoids windowing for spectral representation. We have used the FBSE method for the spectral representation of the analyzed multi-component signals with good frequency resolution. The scale-space based boundary detection method has been applied for the accurate estimation of boundary frequencies in the FBSE based spectrum of the signal. After that, wavelet based filter banks have been generated in order to decompose non-stationary multi-component signals into narrow-band components. Finally, the normalized Hilbert transform has been applied to the estimation of amplitude envelope and instantaneous frequency functions from the narrow-band components and the TF representation of the analyzed non-stationary signal is obtained. We have applied our proposed method for the TF representation of multi-component synthetic signals and real electroencephalogram (EEG) signals.

The proposed method has provided better TF representation as compared to existing EWT method and HHT method, especially when analyzed signal possesses closely spaced frequency components and of short time duration.

List of publications

Journal paper

1. A. Bhattacharyya, L. Singh, and R.B. Pachori, "Fourier-Bessel series expansion based empirical wavelet transform for analysis of non-stationary signals," *Digital Signal Processing*, 78, 185-196, (2018).

Conference paper

1. A. Bhattacharyya, L. Singh, and R.B. Pachori, "Identification of epileptic seizures from scalp EEG signals based on TQWT," *International Conference on Machine Intelligence and Signal Processing*, 22-24 December, 2017, Indore, India.

Contents

List of Figures

List of Abbreviations

AM	Amplitude modulation
AM-FM	Amplitude modulated and frequency modulated
AFM	Amplitude and frequency modulated
CAD	Coronary artery disease
ECG	Electrocardiogram
EEG	Electroencephalogram
EMG	Electromyogram
EMD	Empirical mode decomposition
EWT	Empirical wavelet transform
FB	Fourier-Bessel
FBSE	Fourier-Bessel series expansion
FFT	Fast fourier transform
FM	Frequency modulation
GL	Gaussian-Laguerre
HHT	Hilbert-Huang transform
HT	Hilbert transform
IA	Instantaneous amplitude
IF	Instantaneous frequency
IMFs	Intrinsic mode functions
MSE	Mean square error
MUSIC	Multiple signal classification
NHT	Normalized Hilbert transform
SB	Sub-band
STFT	Short-time fourier transform
TF	Time-frequency
TFDs	Time-frequency distributions
TQWT	Tunable-Q wavelet transform
VMD	Variational mode decomposition
WT	Wavelet transform
WVD	Wigner-Ville distribution

Chapter 1

Introduction

This chapter provides a framework for signal processing i.e. operating in some fashion on a signal to extract some useful information. For example, whenever we hear a sound, our ears and auditory pathways connected to the brain process the sound to extract the information. Thus, the signal is processed by a system. In the example mentioned before, the system is biological in nature. Signal processing can also be defined as an art of representing, transforming, analysing, and manipulating signals. It deals with a wide range of signals, from speech and audio signals to images and video signals, and many others. Signal processing techniques have been found very useful in diverse applications such as speech enhancement [1, 2], image denoising [3, 4], speech analysis [5], digital audio coding [6], image compression [7, 8], radar signal processing [9, 10], and digital communications [11].

1.1 Background and motivation

The objective of typical real-world signal processing application is to explore the behavior of recorded signals [12], and then extract useful information from the signal by transforming it. This technique improves our understanding of the information contained in this signal. The traditional way to analyse a signal is in either time domain analysis or frequency domain analysis. The time domain records system parameters versus time [13]. Analyses of a signal in the time domain make it difficult to provide any information about the distribution of energy over different frequencies and the frequency variations over time [14]. On the other hand, using frequency domain analysis [15], the information about the frequency content of the signal can be easily extracted and analysed. However, the problem with frequency domain analysis is the difficulty to recognize the occurrence of these frequency components with time. An accurate spectrum analysis of such signals cannot be accomplished by the simple use of traditional time-domain representations such as correlation methods or frequency-domain representations based on the Fourier transform. Rather, it requires the use of analysis methods that do not assume any condition of stationarity, as does classical spectrum analysis based on the Fourier transform. For such signals, the concept of time-frequency distributions (TFDs) [16, 17, 18, 19], has been introduced.

1.2 The need for non-stationary signal processing methods

Non-stationary signal analysis methods are focused to model the inherent time-varying characteristics of the analyzed signals recorded in various fields of science and engineering. Moreover, the real-life complicated biological signals [20, 21, 22, 23, 24], finance signals [25], and civil structure vibration signals [26, 27], are highly non-stationary in nature. These signals usually vary with time and require adequate analysis based on their information content. Thus, there is a need to describe how the spectral content of a signal changes with time. In contrast with the time and frequency domains for signal analysis, time-frequency (TF) techniques allow us to analyze the signal in both time and frequency domains. This means that TF techniques show changes of the signals frequency components with respect to time, yielding a potentially more revealing picture of the temporal localization of a signal's spectral components [28]. To overcome the limitations of analysis in the time domain alone or in the frequency domain, a number of TF domain based non-stationary signal analysis methods have been introduced.

1.3 Types of non-stationary signal analysis method

There are serval TF domain based methods available for non-stationary signal analysis in the literature, namely short-time Fourier transform (STFT) [29], wavelet transform (WT) [30], Wigner-Ville distribution (WVD) [31], and Hilbert-Huang transform (HHT) [32]. The features can be extracted in TF domain for the classification of non-stationary signals [33]. The STFT provides TF representation of non-stationary signals based on moving window concept. But, the use of fixed moving window imposes a trade off between time and frequency resolutions in TF plane. In order to overcome the limitations of STFT, the WT was proposed for the efficient TF representation of non-stationary signals.

The WT uses pre-fixed basis functions and decomposes signals into different oscillatory levels with the transient characteristics of the analyzed signals retained [34]. However, due to predefined filter banks, WT fails to decompose signals according to the presence of information content. Therefore, it is difficult to determine instantaneous amplitude (IA) and instantaneous frequency (IF) functions from the decomposed components corresponding to actual mono-component signals. The wavelet packet transforms [35, 36], was proposed in order to enhance signal adaptability. However, this approach is still limited by the use of prefixed basis functions. In [37], authors proposed tunable-Q wavelet transform (TQWT) for the analysis of non-stationary signals. In TQWT method, the Q factor of the wavelet transform can be tuned in accordance with the oscillatory nature of the signal. In [38], authors proposed identification of epileptic seizures from scalp electroencephalogram (EEG) signals based on TQWT. The proposed method clearly detects the epileptic seizure events in scalp EEG records. In [39], authors proposed synchrosqueezed wavelet transform as the combination of WT and reallocation methods. This method achieved better TF resolution as compared to conventional WT. In [40], authors proposed a parametrization technique to design joint time-frequency optimized discrete-time biorthogonal wavelet bases. In [41], authors introduced variational mode decomposition (VMD) method which decomposes a real valued signal into the finite number of components. The VMD method has been found suitable for analysing non-stationary signals and applied in [42], for instantaneous voiced and non-voiced detection from speech signals and in [43], for speech enhancement.

Majority of the existing methods rely on pre-fixed basis functions to analyze the signals and hence are considered to be rigid or non-adaptive. However, the non-adaptive methods face difficulty in analysing physical signals due to the presence of closely spaced frequency components. In the HHT based TF representation [32], empirical mode decomposition (EMD) method adaptively decomposes analyzed signals into amplitude and frequency modulated components known as intrinsic mode functions (IMFs). Later, the Hilbert transform (HT) was applied in each of the IMF for the estimation of IA and IF functions and TF representation was generated. In [45], authors cancelled the occurrences of riding waves from the empirically decomposed frequency modulation (FM) parts of the IMFs. However, the EMD method suffers from mode mixing problem and thus, IF functions cannot be effectively estimated. In [46], authors proposed adaptive Fourier decomposition method in order to decompose non-stationary signals into a number of Fourier intrinsic band functions and provided time-frequency-energy distribution of the analyzed signals. In [47], authors introduced swarm decomposition based on fosters rules of biological swarms for the analysis of non-stationary signals. The method achieved good performance in extracting the components from the analyzed signals. In [48, 49, 50], TF representation was proposed using improved eigenvalue decomposition of the Hankel matrix together with HT for the analysis of non-stationary signals. In [51, 52, 53, 54], authors proposed eigenvalue decomposition for the analysis of electromyogram (EMG) signal, coronary artery disease (CAD) identification, baseline wander and power line interference removal from electrocadioram (ECG) signals. TF representation using WVD is highly affected by the presence of cross-terms between the signal components [55, 56]. This puts a major limitation towards the efficient estimation of IFs of the analyzed signals in multi-component situation.

In [57], empirical wavelet transform (EWT) was proposed for the analysis of non-stationary signals. In [58], authors present several extensions of EWT approach to two-dimensional (2D) signals (images). In [59], the authors explored the EWT method for multivariate signals and EWT based multivariate TF representation was proposed. It should be noted that EWT is an adaptive decomposition method which extracts narrow-band frequency components from the analyzed signal based on the frequency information contained in the signal spectrum. It decomposes signals with adaptive wavelet based filters after finding the boundary frequencies in the fast Fourier transform (FFT) based Fourier spectrum. The TF representation based on EWT can be obtained by applying the HT on the narrow band frequency components. However, EWT fails to represent closely spaced frequency components in the TF plane [60]. Moreover, it is very difficult to estimate the accurate frequency components for the short duration signals using EWT method due to the use of Fourier spectrum.

1.4 Contributions in this work

An improved method is desirable in order to encounter the aforementioned shortcomings of the existing EWT method. In this work, the conventional FFT [61, 62], based Fourier spectrum has been replaced with the spectrum obtained using Fourier-Bessel series expansion (FBSE). It should be noted that, FBSE coefficients are useful for the spectral analysis of non-stationary signals due to the non-stationary nature of Bessel functions bases in the FBSE [63, 64, 65]. We have employed the existing scale-space based boundary detection method for the spectrum segmentation purpose. Finally, the normalized Hilbert transform (NHT) [44], based TF representation has been generated for analysing multi-component non-stationary signals. The proposed method has been applied on synthetically generated multi-component amplitude modulation (AM) and FM signals as well as on real EEG signals. We have obtained better TF representation using proposed FBSE-EWT method as compared to existing EWT and HHT based TF representation for majority of the considered cases.

1.5 Organization of the thesis

The remaining portions of this dissertation are organized in the following way:

- In chapter 2, EWT method, boundary detection through scale-space representation, FBSE and NHT are explained. Plot of an arbitrary Bessel basis function, FFT of the considered basis function, Fourier Bessel (FB) coefficients of the considered Bessel function, and the FBSE spectrum are presented in this chapter. Then, the advantage of NHT over HT through plots of IA and IF using HT and NHT is also presented in this chapter.
- The FBSE based EWT for synthetic multi-component and real EEG signals analysis is explained in chapter 3. The performane evaluation is explained in terms of mean square error (MSE) in this chapter.
- TF representation of synthetic multi-component AM signals, multi-component FM signals and real EEG signals are presented in chapter 4. The performance of TF representation of the proposed method has been also compared with HHT and EWT methods.
- Finally, the whole work is concluded in chapter 5. The directions of future research work are also provided in this chapter.

Chapter 2

Empirical wavelet transform, Fourier-Bessel series expansion, and normalized Hilbert transform methods

Some previous methods like as EMD [32], used to decompose a signal into a set of distinct modes. it is useful in many applications besides lacking mathematical theory. The EMD has three drawbacks, i.e. boundary effect, mode-mixing and stop criteria. In [57], author presented a new approach to build adaptive wavelets. The idea behind this method is to extract the different modes from the signal by designing a suitable wavelet filter bank. This formation leads to a new wavelet transform called EWT. We have used scale-space based boundary detection method which work on the concept of local minima [66]. The FFT spectrum has been replaced with FBSE spectrum for the estimation of optimal boundary frequencies and improved wavelet based filter bank has been obtained. FBSE uses Bessel functions as basis functions, which are damped in nature this makes FBSE suitable for non-stationary signal analysis. We have used NHT for computation of the IA and IF throughout this work because NHT provides better IF estimation of the considered amplitude and frequency modulated (AFM) signal than HT.

2.1 Empirical wavelet transform

The EWT is an adaptive signal decomposition method which was proposed in [57], for the analysis of non-stationary signals. In [58], authors present several extensions of EWT approach to two-dimensional (2D) signals (images). The inherent mechanism of EWT is based on the formation of adaptive wavelet based filters. These wavelet based filters possess support in the spectrum information location of the analyzed signal. The obtained sub-band signals after EWT decomposition have specific center frequencies with compact frequency supports. The EWT method is summarised in the following steps [57];

1. The FFT method is used to obtain frequency spectrum of the analyzed signal in the frequency range $[0, \pi]$.

2. The frequency spectrum is segmented into N number of contiguous segments using EWT boundary detection method. In this work, we have used scale-space based boundary detection method [66], in order to find optimal set of boundary frequencies denoted as ω_i. In the next subsection, the scale-space based boundary detection method is discussed in brief. It should be noted that, the first and last boundary frequencies are prefixed to 0 and π, respectively. Thus, EWT boundary detection method is used to find the rest of the $N-1$ intermediate boundary frequencies.

3. The empirical scaling and wavelet functions are defined in each segment as the set of band-pass filters. The idea of construction of Littlewood-Paley and Meyer's wavelets is used for the construction of wavelet based filters [30, 57].

The mathematical expressions of empirical scaling function $\Lambda_i(\omega)$ and wavelet function $\Theta_i(\omega)$ have been presented in Table 2.1. In the table, the function $\eta(\xi, \omega_i)$ is expressed as [57],

Table 2.1: Mathematical expressions of EWT scaling and wavelet functions.

Functions	Mathematical representation
Scaling [57]	$\Lambda_i(\omega) = \begin{cases} 1, & \text{if } \lvert\omega\rvert \leq (1-\xi)\omega_i. \\ \cos\left(\frac{\pi\eta(\xi,\omega_i)}{2}\right), & \text{if } (1-\xi)\omega_i \leq \lvert\omega\rvert \leq (1+\xi)\omega_i. \\ 0, & \text{otherwise} \end{cases}$
Wavelet [57]	$\Theta_i(\omega) = \begin{cases} 1, \\ \quad \text{if } (1+\xi)\omega_i \leq \lvert\omega\rvert \leq (1-\xi)\omega_{i+1}. \\ \cos\left(\frac{\pi\eta(\xi,\omega_{i+1})}{2}\right), \\ \quad \text{if } (1-\xi)\omega_{i+1} \leq \lvert\omega\rvert \leq (1+\xi)\omega_{i+1}. \\ \sin\left(\frac{\pi\eta(\xi,\omega_i)}{2}\right), \\ \quad \text{if } (1-\xi)\omega_i \leq \lvert\omega\rvert \leq (1+\xi)\omega_i. \\ 0, \text{otherwise}. \end{cases}$

$$\eta(\xi, \omega_i) = \psi\left(\frac{(|\omega| - (1-\xi)\omega_i)}{2\xi\omega_i}\right) \tag{2.1}$$

where $\psi(z)$ is an arbitrary function defined as [57],

$$\psi(z) = \begin{cases} 0, & \text{if } z \leq 0. \\ \text{and } \psi(z) + \psi(1-z) = 1, & \forall z \in [0 \quad 1] \\ 1, & \text{if } z \geq 1. \end{cases} \tag{2.2}$$

The parameter ξ in Table 2.1 makes sure that empirical wavelets and scaling function form a tight frame in $L_2(R)$. The tight frame condition is expressed as follows [57]:

$$\xi < \min_i \left(\frac{\omega_{i+1} - \omega_i}{\omega_{i+1} + \omega_i}\right) \tag{2.3}$$

Now, the detail and approximation coefficients can be determined by taking the inner product of the analyzed signal with wavelets and scaling function which are expressed as [57],

$$\mathbf{V}_{y,\Theta}(i,t) = \int y(\tau)\overline{\Theta_i(\tau - t)}d\tau \tag{2.4}$$

$$\mathbf{V}_{y,\Lambda}(0,t) = \int y(\tau)\overline{\Lambda_1(\tau - t)}d\tau \tag{2.5}$$

where $\mathbf{V}_{y,\Theta}(i,t)$ denotes the detail coefficients of i^{th} oscillatory level, whereas $\mathbf{V}_{y,\Lambda}(0,t)$ denotes the approximation coefficients.

Finally, the reconstructed sub-band signals can be defined as [57],

$$f_0(t) = \mathbf{V}_{y,\Lambda}(0,t) \star \Lambda_1(t) \tag{2.6}$$

$$f_i(t) = \mathbf{V}_{y,\Theta}(i,t) \star \Theta_i(t) \tag{2.7}$$

where $f_0(t)$ is the approximation subband signal and $f_i(t)$ denotes detail subband signal of i^{th} level. The asterisk symbol denotes convolution operation in eqns (2.6) and (2.7).

2.2 Boundary detection based on scale-space representation

The scale-space representation of a discrete signal $x(n)$ can be obtained by computing the convolution of the signal with the Gaussian kernel, which is expressed as [66]

$$\Upsilon(m,t) = \sum_{n=-M}^{M} x(m-n)f(n;t) \tag{2.8}$$

where,

$$f(n;t) = \frac{1}{\sqrt{2\pi t}}\mathrm{e}^{\frac{-n^2}{2t}} \tag{2.9}$$

where $M = D\sqrt{t} + 1$ with $3 \leq D \leq 6$ and t is known as scale parameter. It should be noted that, as the scale parameter or scale-step parameter ($\rho = \sqrt{\frac{t}{t_o}}$,

$\rho = 1, 2, \dots \rho_{\max}$) increases, the number of minima decreases in the scale space plane and no new minima appears. Let the total number of initial minima is denoted by N_0. Thus, each of the initial minima P_i leads to a curve D_i in the scale-space plane of length R_i, where i varies from 1 to N_0. The length (integer) R_i is considered as life time of minima i (not equal to the arc length of D_i) and expressed as $R_i = \max\{\rho/\text{the } i^{\text{th}} \text{ minimum exists}\}$. Using this concept, the meaningful modes are defined in the histogram, as follows: The support of a meaningful mode should be delimited by two local minima which lead to two long (greater than a threshold T_h) scale-space curves D_i. Therefore, the optimal threshold (T_h) should be determined in order to select the scale-space curves of length higher than threshold value [67]. Finally, the Ostu's method [68], has been used for determining the threshold value T_h and meaningful modes have been found.

2.3 Fourier-Bessel series expansion

The FBSE uses Bessel functions as bases, which are non-stationary in nature and it is suitable for analysis of non-stationary signals.

The FBSE of $y(n)$ using zero-order Bessel functions is expressed as follows [69, 70, 71]:

$$y(n) = \sum_{i=1}^{U} C_i J_0\left(\frac{\beta_i n}{U}\right), \ n = 0, 1, \dots, U-1 \tag{2.10}$$

where, C_i are known as the Fourier-Bessel (FB) series coefficients of $y(n)$ which can be expressed as follows [69, 70]:

$$C_i = \frac{2}{U^2(J_1(\beta_i))^2} \sum_{i=1}^{U} n y(n) J_0\left(\frac{\beta_i n}{U}\right) \tag{2.11}$$

where, $J_0(.)$ and $J_1(.)$ denote zero and first-order Bessel functions, respectively. The positive roots (in the ascending order) of the zero-order Bessel function ($J_0(\beta) = 0$) are denoted by β_i with $i = 1, 2, \cdots U$. It should be noted that, order i of the FB series coefficients is related to continuous time frequency f_i (in Hz) where it has the peak value, by the following equation [69, 70]:

$$\beta_i \approx \frac{2\pi f_i U}{f_s}, \text{ where } \beta_i \approx \beta_{i-1} + \pi \approx i\pi \tag{2.12}$$

In equation (2.12), f_s denotes the sampling frequency.

The equation (2.12) can be expressed as [70, 72],

$$i \approx \frac{2 f_i U}{f_s} \tag{2.13}$$

Hence, it is clear from equation (2.13) that, i should be varied from 1 to U (discrete-time signal length) in order to cover the entire bandwidth of the analyzed discrete-time signal. Thus, FBSE spectrum is the plot of magnitude of the FB coefficients ($|C_i|$) versus frequencies (f_i).

The spectral representation using FBSE has some advantages over conventional FFT based spectral representation, such as,

Firstly, FBSE spectrum has compact representation as compared to conventional Fourier representation [73, 74, 75, 64]. Fig. 2.1(i) presents the plot of an arbitrary Bessel basis function $\left(J_0\left(\frac{\beta_{150} n}{U}\right),\ U = 1400\right)$ with 200 Hz sampling frequency. Figure 2.1(ii) shows its Fourier spectrum. It can be seen in the figure that Bessel function has time varying amplitude (decays with time). In [76] authors found that effective bandwidth of a signal is the contribution from AM bandwidth and FM bandwidth. Thus, a significant part of the total bandwidth of a Bessel function arises due to its AM nature. As a result, they have specific center frequency with finite bandwidth in the FFT spectrum. This is in contrast to sinusoidal basis functions of the Fourier transform, which do not contain AM and represented by spectral lines only. Fig 2.1(iii) and (iv) show the plots of FBSE coefficients versus their orders and frequencies, respectively. It is clearly visible that the same finite bandwidth signal is represented by a single coefficient in FBSE domain. On the other side, it is obvious that a sinusoidal wave which is a basis function in Fourier transform, will

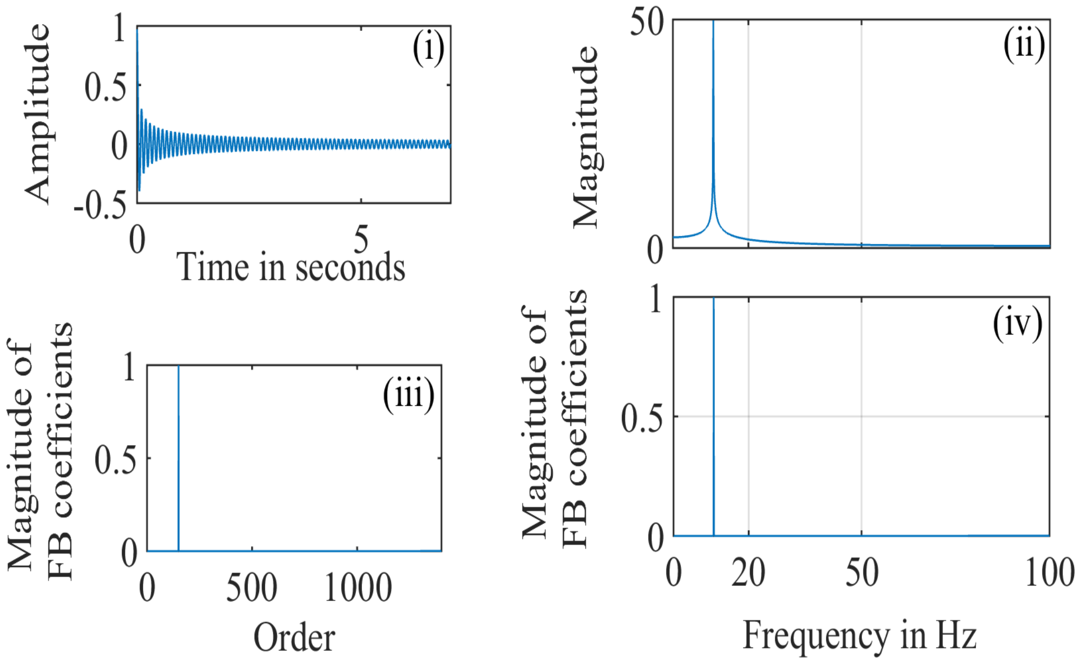

Figure 2.1: (i) Plot of an arbitrary Bessel basis function (ii) Plot of FFT of the considered Bessel basis function (iii) Plot of FB coefficients of the considered Bessel basis function, (iv) Plot of the FBSE spectrum.

be more compactly represented in the FFT domain as compared to FBSE domain due to similarity of basis function with the analyzed signal. In that scenario, more FB coefficients are necessary for the representation of sinusoidal signals. However, real life signals like speech can be represented in terms of amplitude modulated and frequency modulated (AM-FM) components [77, 78]. Such modelling approach is useful to represent wide-band signal in terms of narrow-band signals (AM-FM components). As shown in Figure 2.1, the basis function which is used in FBSE has narrow-band nature in FFT domain and represented compactly in FBSE domain. Such property helps to obtain more compact representation in FBSE domain as compared to FFT domain for wide-band and non-stationary signals. This is because of the contribution of band of frequencies in the representation using Bessel basis functions in the FBSE. On the other hand, in FFT based spectrum, sinusoidal basis functions represent spectral lines which do not have any finite bandwidth in frequency domain. Due to this reason FFT based spectrum is expected to have less compact representation as compared to FBSE spectrum. Hence, it is more likely that a band-pass signal will have more compact representation with fewer non-zero real FB coefficients in the FBSE spectrum.

Secondly, FBSE spectrum avoids the effect of windowing for spectral representation [70]. The FFT based spectral representation is embedded with window function in order to reduce the effect of spectral leakage. However, the multiplication of the window function with signal produces AM and end points distortion in the time domain. On the other hand, FBSE spectrum can produce signal characteristics even for short duration signals without the effect of windowing.

Moreover, spectral representation using FBSE requires the number of coefficients equal to the length of the discrete signal. This is contrary to the conventional FFT spectrum where the spectrum length is half of the analyzed discrete signal [64]. Thus, FBSE based spectrum provides better spectral resolution as compared to FFT spectrum. The zero padding with signal for obtaining same length FFT spectrum will produce only interpolated spectrum with smoother appearance. In practice, the resolution of the transform does not improve since number of points which provides the actual information remains same [79]. The extra points appearing in the FFT spectrum after zero padding will not provide any extra spectral information of the signal. They will be simply interpolated values. In case of FBSE spectrum, all the FB coefficients are unique for the analyzed signal [80, 82].

These features of the FBSE spectrum help us to determine the optimal boundary frequencies more accurately as compared to FFT spectrum, especially when the signal is of short length and contains closed frequency components.

2.4 Normalized Hilbert transform

The HT is used to compute IA and IF functions from the narrow band signal components. The analytic signal representation using HT of narrow-band AFM signal $y(t)$ is expressed as [32],

$$y_h(t) = y(t) + jH[y(t)] \tag{2.14}$$

where, H is the HT operator.

In another way equation (2.14) is represented as,

$$y_h(t) = A(t)e^{j\phi(t)} \tag{2.15}$$

The IA function $A(t)$ and instantaneous phase $\phi(t)$ are represented as,

$$A(t) = \sqrt{y^2(t) + (H[y(t)])^2} \tag{2.16}$$

$$\phi(t) = \arctan\left(\frac{H[y(t)]}{y(t)}\right) \tag{2.17}$$

The IF function $f(t)$ is represented as,

$$f(t) = \frac{1}{2\pi}\frac{d}{dt}[\phi(t)] \tag{2.18}$$

However, Nuttall and Bedrosian in [83], imposed an important condition for getting a meaningful analytic signal for IF computation. This imposes a limitation of separating the HT of the carrier signal from its own envelope, expressed as,

$$H\{\alpha(t)\cos(\theta(t))\} = \alpha(t)H\{\cos(\theta(t))\} \tag{2.19}$$

provided that Fourier transform of the carrier signal and its envelope do not overlap. Thus the signal has to be mono-component and narrow-band as well. Otherwise, the FM part will be contaminated with AM variations. Thus, eqns. (2.14) to (2.18) become no longer valid when the analyzed signal violates the condition mentioned in eqn (2.19).

In [44], the authors proposed NHT in order to get rid of Bedrosian condition [83]. They empirically decomposed AFM signals into envelope (AM) and carrier

(FM) parts. The empirical AM-FM decomposition is summarised as follows [44]:

It requires identification of all the local maxima points from the absolute value of given AFM signal $y(t)$ and connect them with a cubic spline. This spline curve $e_1(t)$ is termed as the envelope of the signal. Now, this obtained envelope is used to normalize the signal $y(t)$. The normalized signal $s_1(t)$ can be expressed as,

$$s_1(t) = \frac{y(t)}{e_1(t)} \tag{2.20}$$

After normalization, the signal $s_1(t)$ should satisfy the condition $|s_1(t)| \leq 1$. Otherwise, the envelope $e_2(t)$ of the signal $s_1(t)$ is found and the normalization process is again repeated, which is expressed as,

$$s_2(t) = \frac{s_1(t)}{e_2(t)} \tag{2.21}$$

After n^{th} iteration, the signal $s_n(t)$ satisfies the condition $|s_n(t)| \leq 1$ and the normalization process is complete. Then, $s_n(t)$ is designated as empirically found FM part $F(t)$ of the AFM signal $y(t)$.

$$F(t) = s_n(t) = \cos(\phi(t)) \tag{2.22}$$

Then, the AM part $A(t)$ of the AFM signal is determined as,

$$A(t) = e_1(t)e_2(t)\dots e_n(t) \tag{2.23}$$

Finally, the AFM signal $y(t)$ is expressed as,

$$y(t) = A(t)F(t) = A(t)\cos(\phi(t)) \tag{2.24}$$

Now, as the empirically obtained FM signal $F(t)$ satisfies $|F(t)| \leq 1$, the condition mentioned in eqn (2.19) is not violated and the computation of analytic signal through Hilbert transform of $F(t)$ is no longer a concern [44]. Thus, IF, $f(t)$ is computed from the FM signal $F(t)$ using analytic signal representation by following eqns (2.14) to (2.18). In Figure 2.2, we have shown the plots of an arbitrary AFM signal and its IAs and IFs using both HT and NHT methods. It can be observed that NHT provides better IF estimation of the considered AFM signal. Thus, we have used NHT for computation of the IA and IF throughout this work.

Finally, the TF coefficients considering all the N oscillatory levels, are expressed as follows [59]:

$$\mathrm{Tf}(f,t) = \sum_{i=1}^{N} A_i(t)\delta[f - f_i(t)] \tag{2.25}$$

where $A_i(t)$ and $f_i(t)$ denote IA and IF functions of i^{th} oscillatory level.

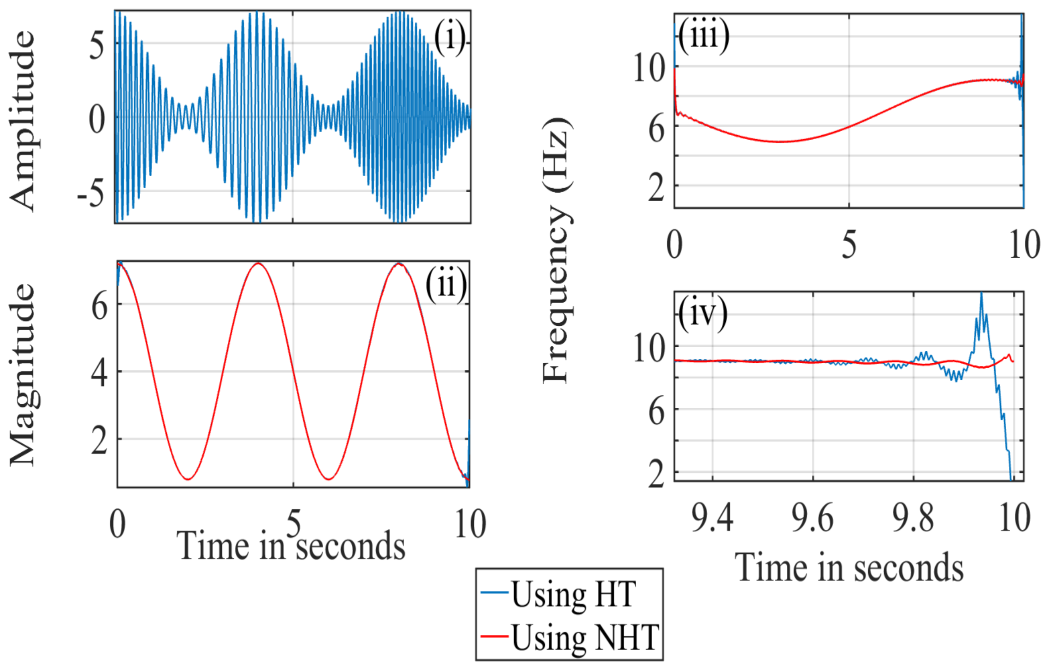

Figure 2.2: (i) Plot of an arbitrary AFM signal $y(t) = 4(1 + 0.8(cos(0.5\pi t))\cos(2\pi(7t + 4\cos(0.52t)))$ with 200 Hz sampling frequency. Plot of (ii) IA and (iii) IF of the signal using HT and NHT methods, (iv) Plot of the zoomed version of the computed IF.

2.5 Summary

In the present work, an alternative method of EMD and EWT has been proposed to realize the signal decomposition by constructing an adaptive filter bank named as FBSE-EWT, for the analysis of non-stationary signals. The mechanism is based on formation of wavelet filter bank. After applying the EWT, obtained sub-band signals contains a specific center frequency. We have replaced the conventional FFT based spectrum with FBSE, as FBSE uses Bessel function as bases which are non-stationary in nature and secondly, FBSE spectrum avoids the effect of windowing for spectral representation. The FFT based spectral representation is embedded with a window function. FBSE spectrum provides a better spectral resolution as compared to FFT. This makes FBSE suitable for non-stationary signals. The scale space based boundary detection method has been used for boundary detection which works on the concept of two local minima. Ostu's method has been used for determining the threshold value. The HT is used to compute IA and IF functions from the narrow band signal components. However, Nuttall and Bedrosian imposed an important condition for getting a meaningful analytic signal for IF computation. In order to get rid of Bedrosian condition, NHT was proposed. The NHT provides better IF estimation of the considered AFM signal. Finally, the NHT based TF representation has been generated for analysing multi-component non-stationary signals.

Chapter 3

Proposed method

In this chapter, we have proposed a method for analysing non-stationary signals. The block diagram of the proposed FBSE-EWT method has been depicted in Figure 3.1.

We have considered synthetic multi-component AM, synthetic multi-component FM, and real EEG signals in the study. First synthetic multi-component AM signal is considered for the experimental purpose with three cases, In the first case, the signal components are very closely spaced in frequency domain. The spacing among the components gradually increased in case two and case three. The reason behind considering the three cases is, whether proposed method can reproduce each of the signal component without interference. We have also considered multi-component FM signal and real epileptic seizure EEG signal for the experimental purpose. The EEG signal used in this thesis is made available publicly by University of Bonn, Germany [84]. Then, the proposed FBSE-EWT based TF representations were compared with existing EWT and HHT based TF (discussed in the introduction section) representation.

In the proposed method, The FBSE is used in order to obtain the frequency spectrum of the analyzed signal. The FFT based spectrum is not used anymore for the boundary detection and spectrum segmentation purpose. FBSE coefficients are useful for the spectral analysis of non-stationary signals because of the non-

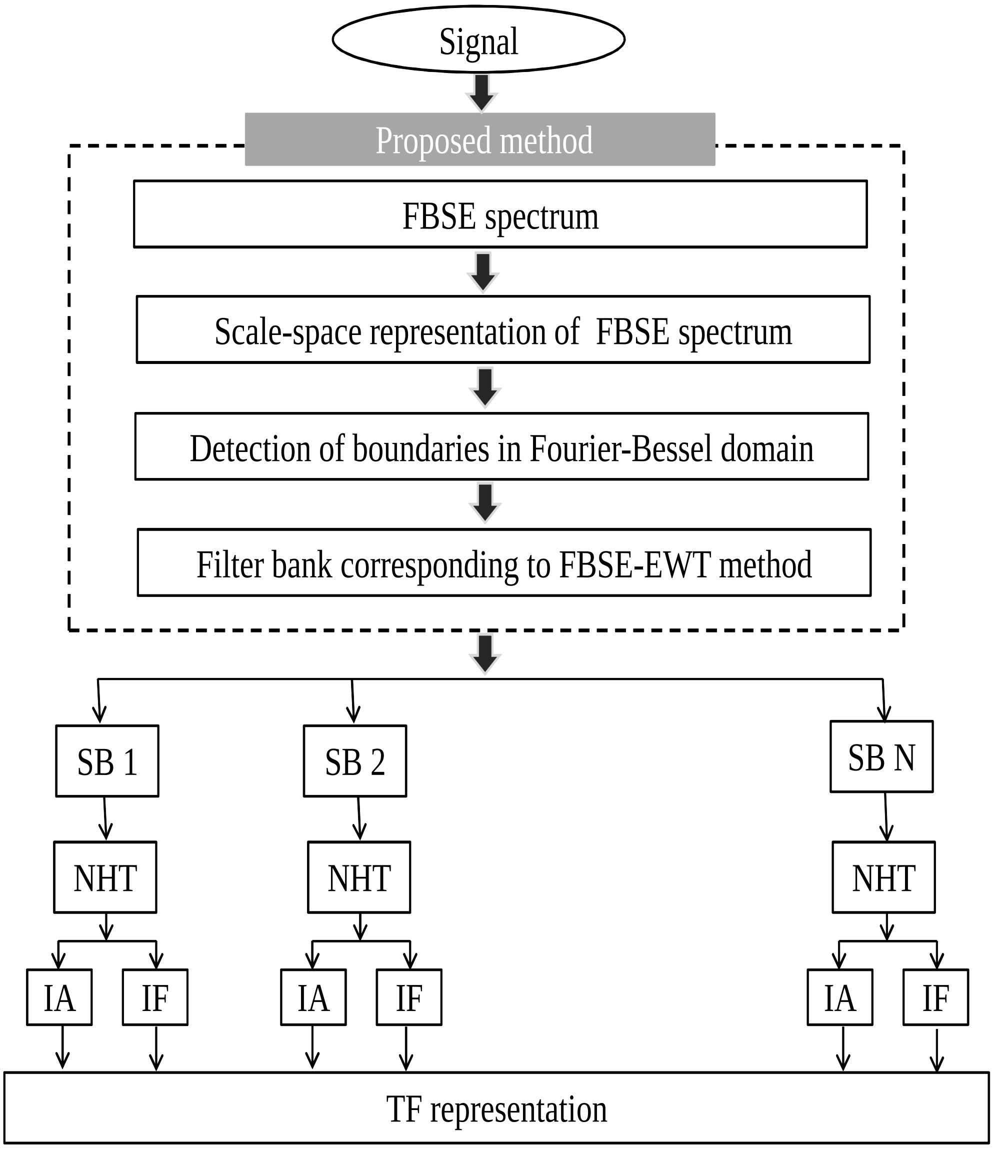

Figure 3.1: Block diagram of the proposed FBSE-EWT based TF representation.

stationary nature of Bessel functions. It has been observed that FBSE spectrum has compact representation as compared to conventional Fourier representation and avoids windowing for spectral representation. Thereafter, scale-space based boundary detection approach was applied to find meaningful modes based on that we have found boundaries and to segment the FBSE spectrum which result in improved EWT based filter bank and sub-band (SB) signals are obtained. The mechanism of EWT is based on the formation of adaptive wavelet-based filters. The wavelet-based filters provide support to the spectrum information location of the analysed signal. The obtained SB signals after EWT decomposition have specific centre frequencies with compact frequency supports.The HT is used to compute IA and IF function from narrowband signals, However, Nuttella and Bedrosian imposed an important condition for getting a meaningful analystic signal for IF computation. This imposes a limitation of separating the HT of the carrier signal. Signal has to be mono-component and narrow-band as well. otherwise FM part will be contaminated with AM variation. in [44], the authors proposed NHT in order to get rid of Bedrosian condition. Thus, In order to obtain the TF representation of analysed signal NHT was applied on each sub-band. Finally, proposed FBSE-EWT based TF representations were compared with existing EWT and HHT based TF (discussed in the introduction section) representations. It should be noted that EWT based TF representations were obtained after applying NHT to the sub-band signals using existing EWT method. For HHT based TF representation, NHT was applied on the IMF's obtained through EMD method.

3.1 Performance evaluation

The performance of the TF representation has been quantitatively measured by computing MSE between the expected TF representation and the obtained TF representation of the considered multi-component synthetic signals (discussed latter). The expected TF representation is obtained by applying NHT to the prior known individual signal components of the considered multi-component synthetic signals. Finally, the MSE is expressed as [81]

$$\mathrm{MSE} = \frac{1}{PQ}\sum_{f=1}^{P}\sum_{t=1}^{Q}(\mathrm{TF}_1(f,t) - \mathrm{TF}(f,t))^2 \tag{3.1}$$

where, P and Q denote the total number of frequency points and total number of time instants in the TF plane, respectively. The TF_1 and TF denote the expected and obtained TF representations, respectively.

3.2 Summary

In this chapter, we have explain the complete methodology for FBSE-EWT. FBSE was applied on multicomponent signals because of its advantage over FFT, FBSE spectrum has twice frequency resolution as compared to FFT spectrum.Thus, it is more advantageous to use FBSE spectrum as compared to FFT spectrum in order to estimate the optimal boundary frequencies. For the boundary detection the scale-space based boundary detection method has been applied. Then, the EWT based filter bank is generated. The sub-band signals after EWT decomposition have specific centre frequencies with compact frequency support. Ostu's method has been used for determining the threshold value. NHT advantages over HT which make NHT suitable for multicomponent signal analysis. NHT has been applied on each sub-band for computation of IA and IF and thus the TF representation was obtained. The performance of TF representation has been quantitatively measured by computing MSE of the expected TF representation and the obtained TF representation of the considered multi-component synthetic signals.

Chapter 4

Simulation results

In this chapter, we have considered multi-component AM and FM signals with three different cases with gradually increasing space betwwen the signal component in frequency domain, we have also considered real EEG signal. Then FBSE-EWT has been applied for the TF representation. The performance of TF representation of the proposed method has also been compared with HHT and EWT methods.

4.1 TF representation of synthetic multi-component AM signals

We have considered synthetic multi-component AM signal expressed as,

$$y(t) = \sum_{i=1}^{3} 0.2(1 + 0.3\cos(2\pi t))\cos(2\pi f_i t)$$

where three different cases have been considered, namely:

Case 1: $f_1 = 9$ Hz, $f_2 = 10$ Hz, $f_3 = 11$ Hz

Case 2: $f_1 = 9$ Hz, $f_2 = 11$ Hz, $f_3 = 13$ Hz

Case 3: $f_1 = 9$ Hz, $f_2 = 12$ Hz, $f_3 = 15$ Hz

In the first case, the signal components are very closely spaced in frequency domain. The frequency spacing among the components have been increased in cases

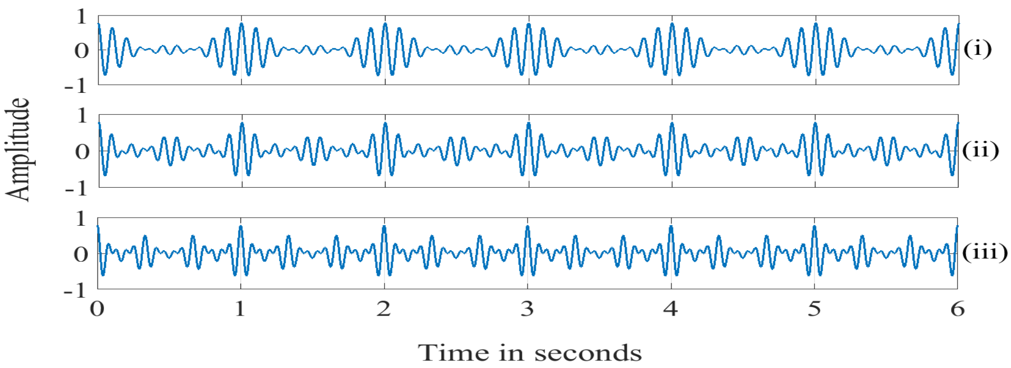

Figure 4.1: Plots of the multi-component AM signals: (i) Case 1, (ii) Case 2, and (iii) Case 3.

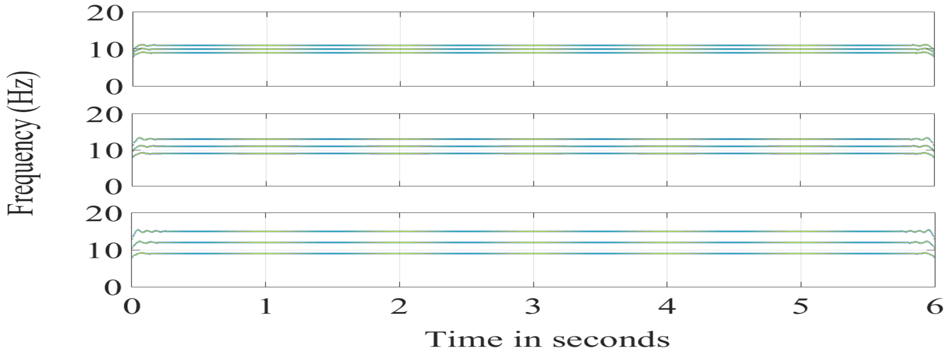

Figure 4.2: Plots of the expected TF representation of multi-component AM signals for Case 1 (top), Case 2 (middle), and Case 3 (bottom).

2 and 3. In all the cases, the signal duration is considered as 6 seconds with a sampling rate of 200 Hz. The multi-component AM signals for all the three cases have been shown in Figure 4.1 and their expected TF representation is shown in Figure 4.2. The intention behind the consideration of the above three cases is, whether the proposed FBSE-EWT method can reproduce each of the signal components in the TF plane without interference. For each of the cases, the performance of the proposed FBSE-EWT method has been compared with HHT and existing EWT method. The obtained TF representations of the three considered cases using HHT method have been shown in Figure 4.3. It can be noticed that, in the first case, the signal components are hardly identifiable. In the second and third cases, three signal components are separable in the TF plane, but they are affected by interference.

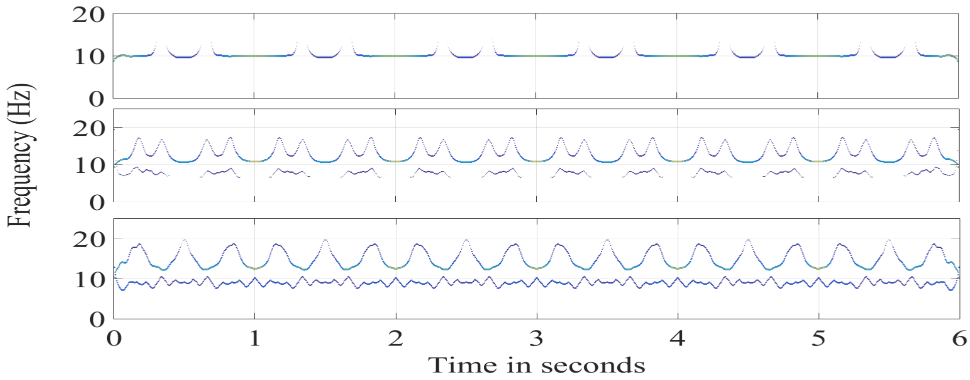

Figure 4.3: Plots of the HHT based TF representation of multi-component AM signal for Case 1 (top), Case 2 (middle), and Case 3 (bottom).

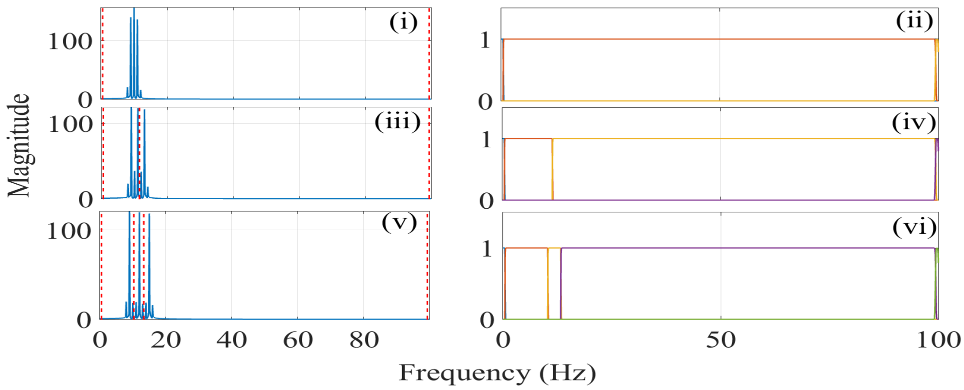

Figure 4.4: Plots of (i) the detected boundaries in the FFT spectrum and (ii) EWT based filter-bank for multi-component AM signal corresponding to Case 1. Plots of (iii) the detected boundaries in the FFT spectrum and (iv) EWT based filter-bank for multi-component AM signal corresponding to Case 2. Plots of (v) the detected boundaries in the FFT spectrum and (vi) EWT based filter-bank for multi-component AM signal corresponding to Case 3.

For EWT based TF representation, the boundary frequencies are not optimally detected in the FFT spectrum when first two cases have been considered, as shown in Figure 4.4 (first column). This resulted into formation of undesired EWT based filter-bank for these two cases (second column of Figure 4.4). The EWT based TF representations for the three considered cases have been presented in Figure 4.5.

It can be observed that, EWT clearly reproduces three individual signal components in the TF plane for the third case only. Thus, EWT method is not able to represent closely spaced frequency components in the TF plane. For all the three cases, the detected boundaries in the FBSE domain and FBSE-EWT based filter

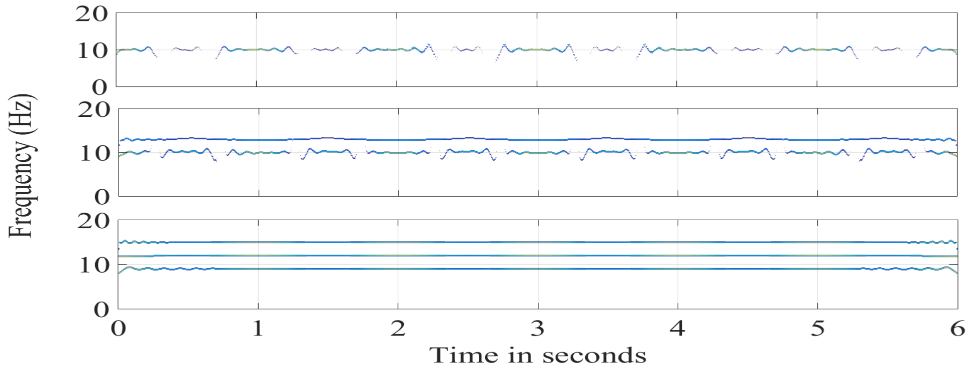

Figure 4.5: Plots of EWT based TF representations of multi-component AM signals corresponding to case 1 (top), case 2 (middle), and case 3 (bottom).

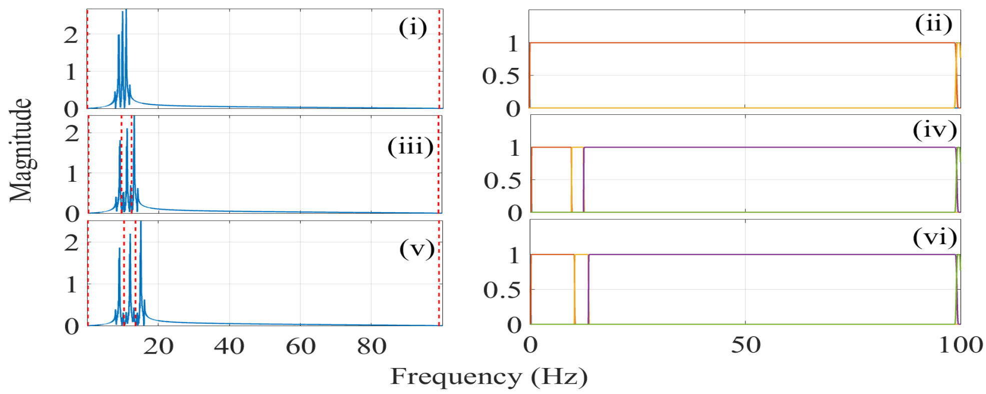

Figure 4.6: Plots of (i) the detected boundaries in the FBSE spectrum, (ii) FBSE-EWT based filter-bank for multi-component AM signal corresponding to Case 1. Plots of (iii) the detected boundaries in the FBSE spectrum and (iv) FBSE-EWT based filter-bank for multi-component AM signal corresponding to Case 2. Plots of (v) the detected boundaries in the FBSE spectrum and (vi) FBSE-EWT based filter-bank for multi-component AM signal corresponding to Case 3.

banks have been presented in first and second column of Figure 4.6, respectively. It can be seen in the figure that, for case 2, the boundary frequencies are optimally detected in the FBSE domain as compared to in FFT domain (shown in Figure 4.4). This is due to the fact that, FBSE spectrum provides better frequency resolution as compared to FFT spectrum. The TF representation of all the three considered cases, using proposed FBSE-EWT method has been presented in Figure 4.7. It is clear from the figures that, except for the first case, proposed FBSE-EWT method clearly represents all the signal components in the TF plane. Thus, for case 1, none of the methods is able to represent the frequency components in the TF plane. Table

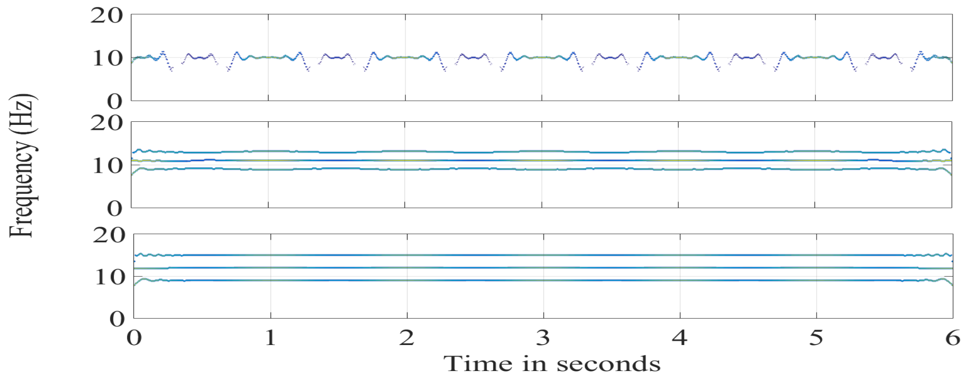

Figure 4.7: Plots of FBSE-EWT based TF representation of multi-component AM signals corresponding to case 1 (top), case 2 (middle), and case 3 (bottom).

Table 4.1: Comparison of the MSE values of multi-component AM signal for different considered cases using FBSE-EWT, EWT, and HHT methods

Cases	FBSE-EWT	EWT	HHT
Case 1	3.924×10^{-4}	3.973×10^{-4}	2.837×10^{-4}
Case 2	1.983×10^{-4}	3.794×10^{-4}	3.742×10^{-4}
Case 3	2.972×10^{-5}	3.66×10^{-5}	3.662×10^{-4}

4.1, presents the MSE values for the HHT, EWT, and proposed FBSE-EWT method when above mentioned three cases of the multi-component AM signals have been considered. For case 1, the MSE values are not considerable as none of the methods was successful in representing multi-component AM signal. For case 2, the MSE values for FBSE-EWT method is the lowest followed by EWT and HHT methods. Such kind of results were expected. For case 3, the MSE value for FBSE-EWT method is lower then EWT based method, whereas MSE for EMD method was the highest. This is because, the TF representation using EMD method has spurious or unwanted frequencies and interference terms which give rise to higher MSE value.

In order to observe the effect of signal duration in the detection of optimal boundary frequencies, we have increased the signal duration of the case 1 multi-component AM signal and considered three different subcases as follows: *subcase 1*: signal duration of 15 seconds, *subcase 2*: signal duration of 20 seconds, and *subcase 3*: signal duration of 25 seconds. The TF representation using HHT method for three different subcases have been shown in Figure 4.8.

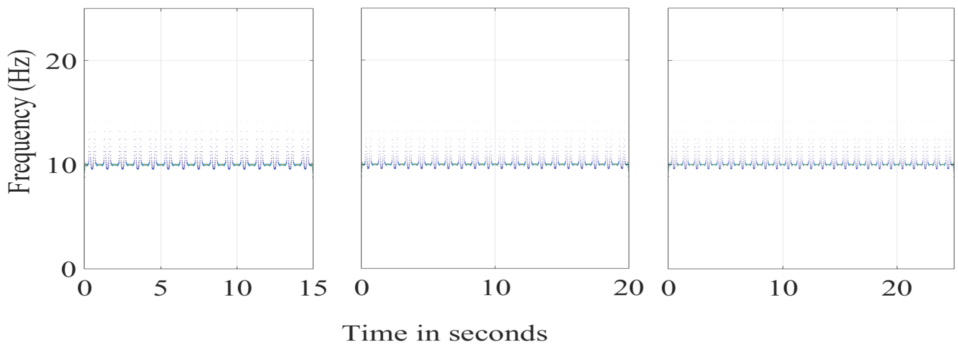

Figure 4.8: Plots of the HHT based TF representation of multi-component AM signals for *subcase 1* (left most), *subcase 2* (middle), and *subcase 3* (right most).

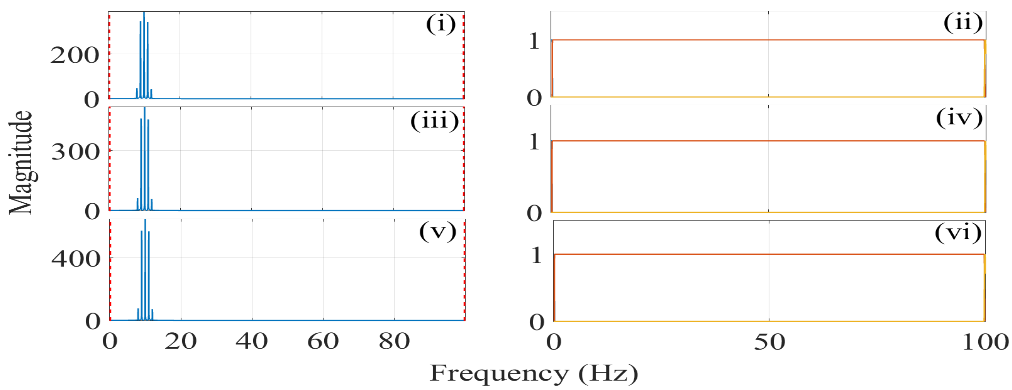

Figure 4.9: Plots of (i) the detected boundaries in the FFT spectrum and (ii) EWT based filter-bank of multi-component AM signal for *subcase 1*. Plots of the (iii) detected boundaries in the FFT spectrum and (iv) EWT based filter-bank of multi-component AM signal for *subcase 2*. Plots of (v) the detected boundaries in the FFT spectrum and (vi) EWT based filter-bank of multi-component AM signal for *subcase 3*.

It can be observed that signal components overlap with each other in the TF plane. Thus, HHT method fails to represent closely spaced frequency components in the TF plane. For each of the considered subcases, the detected boundaries in the FFT spectrum and EWT based filter banks have been shown in the first and second columns of Figure 4.9. It is clear from the figure that boundaries are erroneously detected which resulted into formation of undesired EWT based filter bank. The TF representations using EWT method for the above mentioned subcases have been presented in Figure 4.10. Hence, EWT method is not able to represent the closely spaced frequency components, even for increased signal durations.

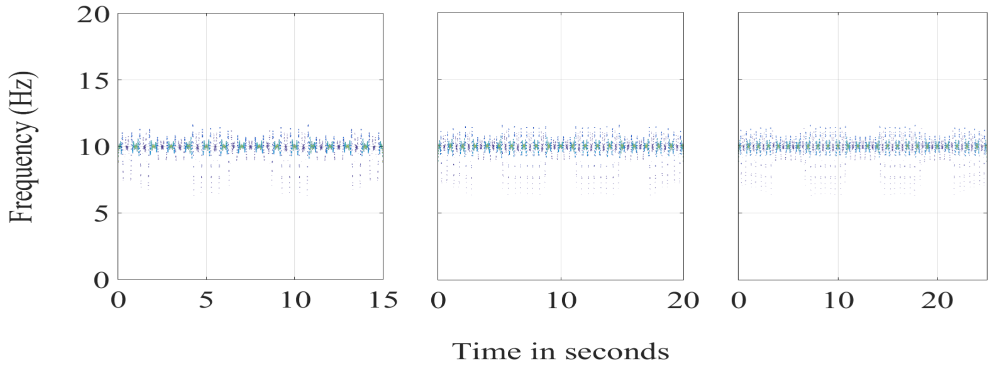

Figure 4.10: Plots of EWT based TF representation of multi-component AM signals corresponding to *subcase 1* (left most), *subcase 2* (middle), and *subcase 3* (right most).

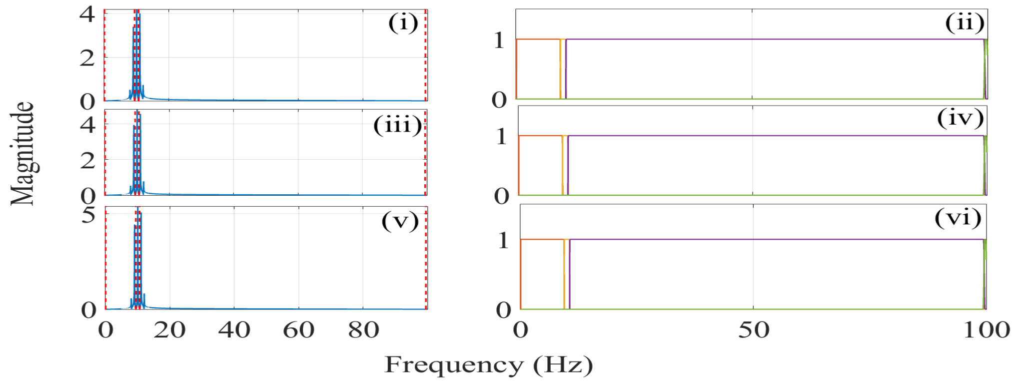

Figure 4.11: Plots of the (i) detected boundaries in the FBSE spectrum and (ii) FBSE-EWT based filter-bank for multi-component AM signal corresponding to *subcase 1*. Plots of (iii) the detected boundaries in the FBSE spectrum and (iv) FBSE-EWT based filter-bank for multi-component AM signal corresponding to *subcase 2*. Plots of (v) the detected boundaries in the FBSE spectrum and (vi) FBSE-EWT based filter-bank for multi-component FM signal corresponding to *subcase 3*.

The detected boundary frequencies in the FBSE domain for all three subcases have been shown in the first column, where as the corresponding filter banks have been presented in the second column of Figure 4.11. The figure shows that optimal boundary frequencies have been detected in the FBSE domain even for closely spaced frequency components. However, it can be noticed in Figures 4.9 and 4.11

that, for all the considered subcases, though FFT based spectrum also has three signal components like as FBSE spectrum, but the optimal boundary frequencies are detected in the FBSE spectrum only.

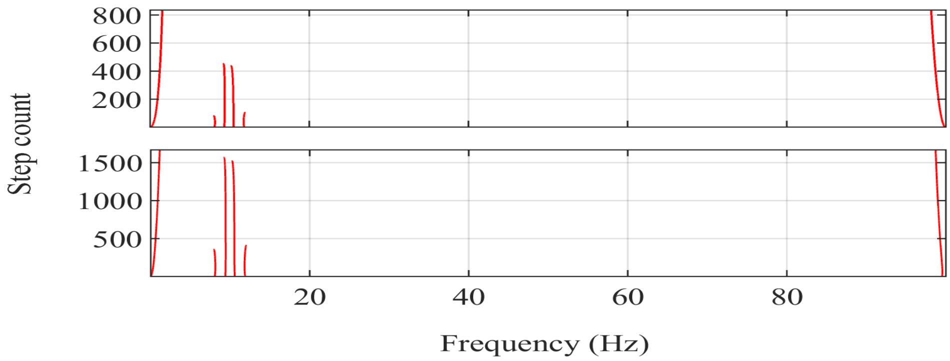

Figure 4.12: Plots of scalespace planes for FFT (top) and FBSE (bottom) spectrums corresponding to *subcase 3*.

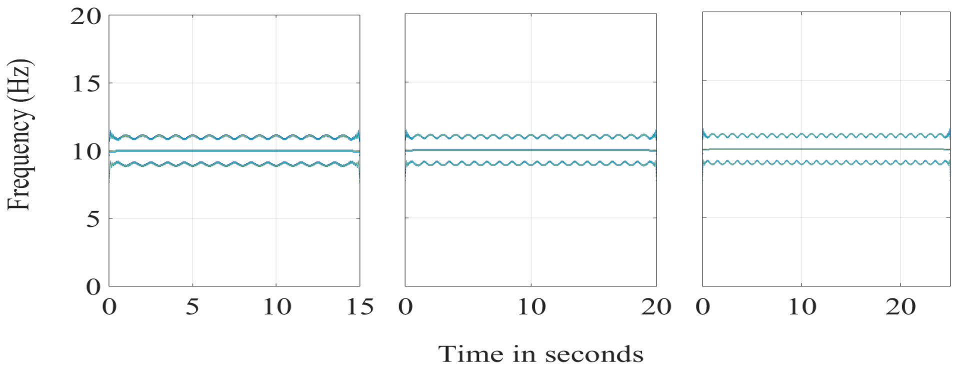

Figure 4.13: Plots of FBSE-EWT based TF representation of multi-component AM signals corresponding to *subcase 1* (left most), *subcase 2* (middle), and *subcase 3* (right most).

The reason is explained with Figure 4.12, which presents the plots of scalespace planes for the FFT and FBSE spectrums corresponding to subcase 3. It is clear in the figure that in both the spectrums, six initial minima points are detected. This led to six scalespace curves (located at initial minima points) of different lengths in each of the scalespace plane. However, after length based thresholding operation, only first (located around zero frequency) and last (located around maximum frequency) scalespace curves are retained in the scalespace plane of FFT spectrum.

Table 4.2: Comparison of the MSE values of multi-component AM signal for different considered subcases using FBSE-EWT, EWT, and HHT methods

Subcases	FBSE-EWT	EWT	HHT
Subcase 1	1.126×10^{-4}	1.797×10^{-4}	1.327×10^{-4}
Subcase 2	9.399×10^{-5}	1.402×10^{-4}	1.012×10^{-4}
Subcase 3	7.29×10^{-5}	1.141×10^{-4}	8.204×10^{-5}

Thus, scalespace method detects only two boundary frequencies (corresponding to location of retained scalespace curves) and fails to detect other two desired boundary frequencies in the FFT spectrum. This is in contrast to FBSE spectrum, where, four scalespace curves are chosen after thresholding. Thus, in FBSE spectrum four boundary frequencies are detected which include two desired boundary frequencies in between the closely spaced frequency components (9 Hz, 10 Hz, and 11 Hz). The TF representations for all the considered subcases using FBSE-EWT method are presented in Figure 4.13 which clearly represent closely spaced frequency components in the TF plane. Thus, proposed FBSE-EWT provides better TF representation for the above considered subcases in comparison to HHT and existing EWT methods. Table 4.2 presents the MSE values for FBSE-EWT, EWT, and HHT based TF representations considering all the three subcases. As expected, the MSE values for FBSE-EWT based TF representation have been found lower in value as compared to HHT and EWT based TF representation for all the subcases.

4.2 TF representation of synthetic multi-component FM signals

In this subsection, we have considered a multi-component FM signal $y(t)$ expressed as,

$y(t) = y_1(t) + y_2(t)$

where $y_1(t)$ is a sinusoidally FM signal and $y_2(t)$ is a linearly FM chirp signal.

These signals are mathematically expressed as

$y_1(t) = \cos\left(2\pi(20t + 4\cos(0.54t))\right)$

$y_2(t) = \cos\left(2\pi(f_4 t + 0.4t^2)\right)$

where three distinct cases have been considered as,

Case 1: $f_4 = 9$ Hz.

Case 2: $f_4 = 10$ Hz.

Case 3: $f_4 = 11$ Hz.

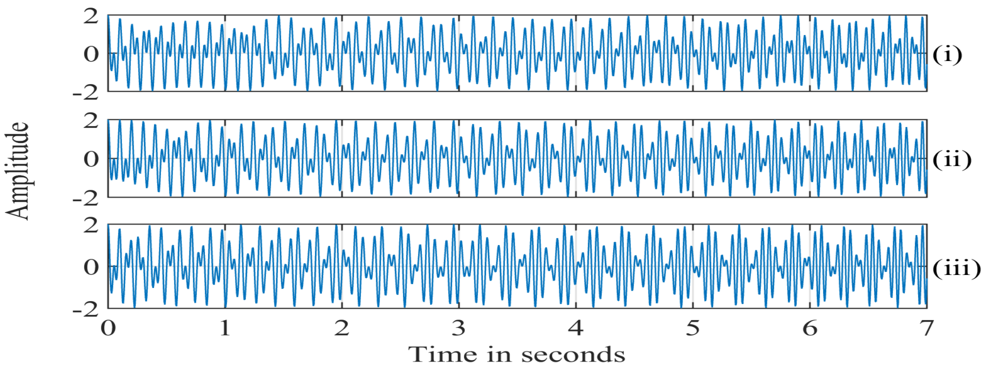

Figure 4.14: Plots of the multi-component FM signals: (i) Case 1, (ii) Case 2, and (iii) Case 3.

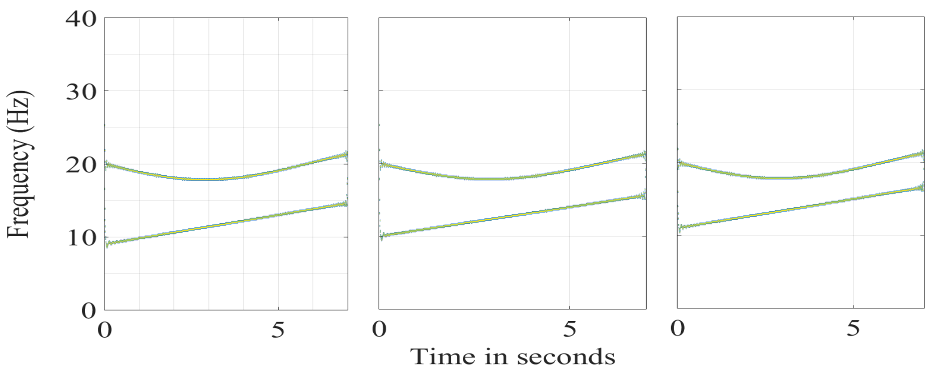

Figure 4.15: Plots of the expected TF representation of multi-component FM signals corresponding to case 1 (left most), case 2 (middle), and case 3 (right most).

In case 1, the signal components $y_1(t)$ and $y_2(t)$ have comparatively higher frequency spacing as compared to Case 2 and Case 3. The frequency spacing between $y_1(t)$ and $y_2(t)$ is the lowest in Case 3 among the three cases. In all the cases, we have considered signal duration of 7 seconds with a sampling rate of 200 Hz. The syn-

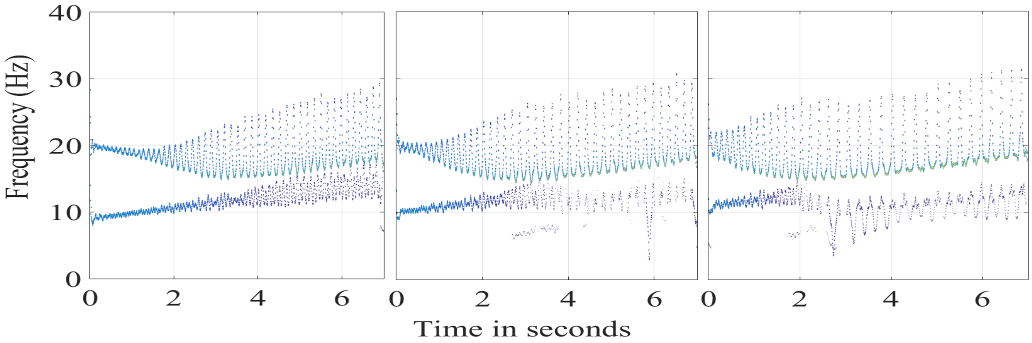

Figure 4.16: Plots of HHT based TF representation of multi-component FM signals corresponding to case 1 (left most), case 2 (middle), and case 3 (right most).

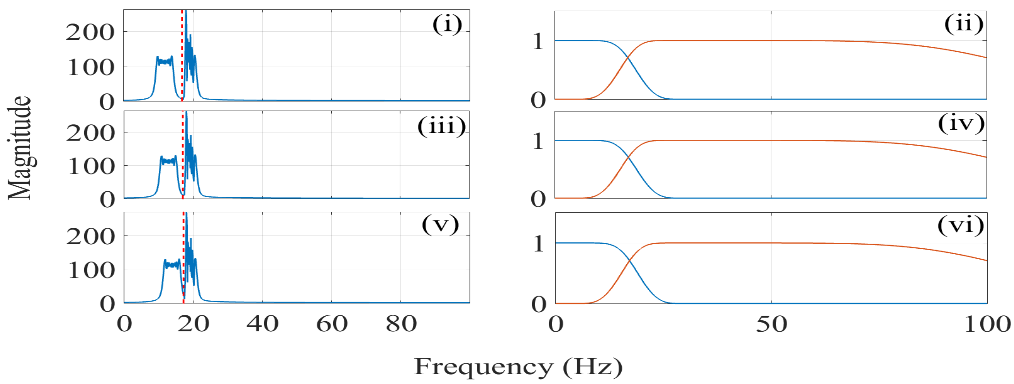

Figure 4.17: Plots of (i) the detected boundaries in the FFT spectrum and (ii) EWT based filter-bank for multi-component FM signal corresponding to Case 1. Plots of (iii) the detected boundaries in the FFT spectrum and (iv) EWT based filter-bank for multi-component FM signal corresponding to Case 2. Plots of (v) the detected boundaries in the FFT spectrum and(vi) EWT based filter-bank for multi-component FM signal corresponding to Case 3.

thetic multi-component FM signals corresponding to all the cases have been shown in Figure 4.14 and their expected TF representations are depicted in Figure 4.15. We have generated TF plane for all the three cases using the proposed FBSE-EWT method as well as with existing HHT and EWT methods. Figure 4.16 presents the HHT based TF representation corresponding to three considered cases of multi-component FM signals. It can be observed from the figure that, HHT based TF representation suffers from interference terms. This is because of the mode mixing problem encountered by EMD method and the computation of IFs become difficult. Figure 4.17 presents the detected boundaries in the FFT spectrum (first column),

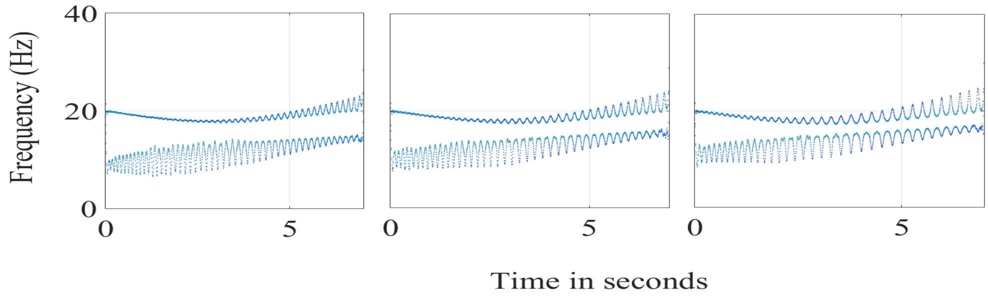

Figure 4.18: Plots of EWT based TF representation of multi-component FM signals corresponding to case 1 (left most), case 2 (middle), and case 3 (right most).

Table 4.3: Comparison of the MSE values of multi-component FM signal for different considered cases using FBSE-EWT, EWT, and HHT methods

Cases	FBSE-EWT	EWT	HHT
Case 1	0.0015	0.0043	0.0048
Case 2	0.0015	0.0044	0.0051
Case 3	0.0015	0.0045	0.0053

and the generated filter banks (second column) corresponding to the three considered cases. The EWT based TF representation corresponding to above three cases of multi-component FM signals have been presented in Figure 4.18. It can be noticed that EWT method has provided better TF representation as compared to HHT representation. However, the EWT based TF representation is not completely free from the presence of interference terms in the TF plane. The detected boundaries in the FBSE domain and the formed FBSE-EWT filter banks are shown in the first and second column of the Figure 4.19, respectively. The TF representation based on FBSE-EWT method corresponding to three considered cases have been presented in Figure 4.20.

It can be observed from the figure that, FBSE-EWT method clearly represents the multi-component FM signals in the TF plane. Table 4.3 presents the MSE values of all the studied TF representation methods for all the considered cases. It can be observed that, the MSE values for the proposed FBSE-EWT method are less in

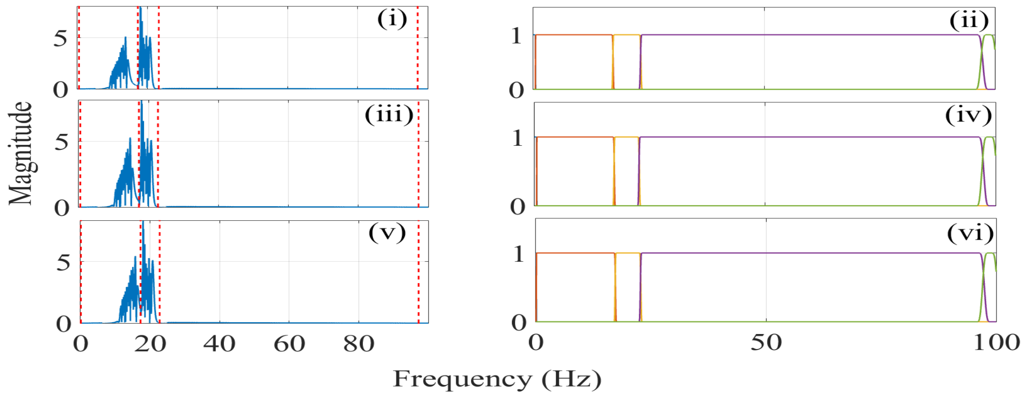

Figure 4.19: Plots of (i) the detected boundaries in the FBSE spectrum, (ii) FBSE-EWT based filter-bank for multi-component FM signal corresponding to Case 1. Plots of (iii) the detected boundaries in the FBSE spectrum and (iv) FBSE-EWT based filter-bank for multi-component FM signal corresponding to Case 2. Plots of (v) the detected boundaries in the FBSE spectrum and (vi) FBSE-EWT based filter-bank for multi-component FM signal corresponding to Case 3.

comparison to HHT, and EWT methods. These results are corresponding to the obtained TF representations using FBSE-EWT, EWT, and HHT methods.

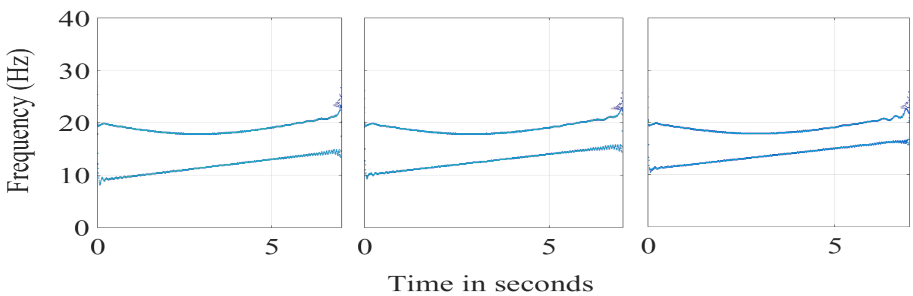

Figure 4.20: Plots of FBSE-EWT based TF representation of multi-component FM signals corresponding to case 1 (left most), case 2 (middle), and case 3 (right most).

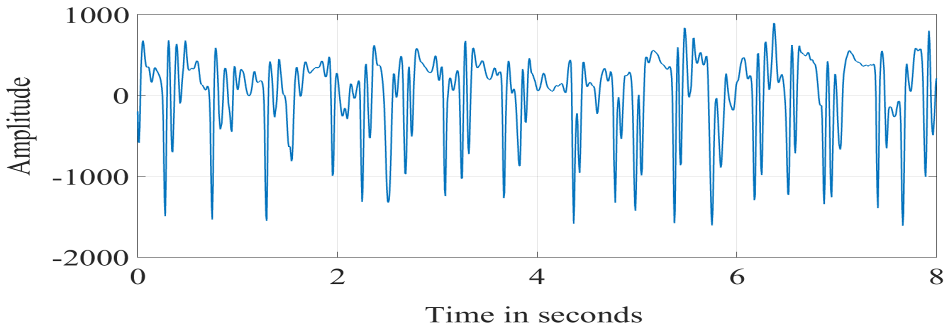

Figure 4.21: Plot of real EEG signal.

4.3 TF representation of real electroencephalogram signals

We have applied the proposed FBSE-EWT method for the TF representation of real epileptic seizure EEG signal. The EEG signal used in this paper is made available publicly by University of Bonn, Germany [84]. The EEG signal has a sampling rate of 173.61 Hz with a duration of 23.6 seconds. In this work, we have obtained the TF representation of the 8 seconds duration segment of the EEG signal, as shown in Figure 4.21. The TF representation using FBSE-EWT method has been compared with HHT and existing EWT method. It can be seen from the Figure 4.22 that, HHT based TF representation generates spurious frequencies in TF plane and suffers from interference. The EWT based TF representation has been shown in Figure 4.23(iii), where as the detected boundaries in the FFT spectrum and EWT based filter banks for the real EEG signal have been shown in Figure 4.23(i) and (ii), respectively. It is clear from the figure that EWT method generates unwanted and mostly scattered IFs. This is because, some of the EWT generated sub-band signals are wide band frequency components due to improper detection of boundary frequencies in the FFT spectrum. The detected boundaries in the FBSE domain, the FBSE-EWT based filter bank and obtained FBSE-EWT based TF representation have been shown in Figure 4.24 (i), (ii), and (iii), respectively. It should be noted that almost all the subband signals generated using FBSE-EWT method are narrow-band in nature. This helps to compute the more meaningful IF using NHT. In HHT and EWT based TF representations, it is difficult to interpret the frequency components above 15 Hz as they are mostly scattered and not well connected. However, the FBSE-EWT provides more clear TF representation of the frequency components in low as well as in high frequency regions. Thus, FBSE-EWT has clear advantage over EWT and HHT in the TF representation of non-stationary signals.

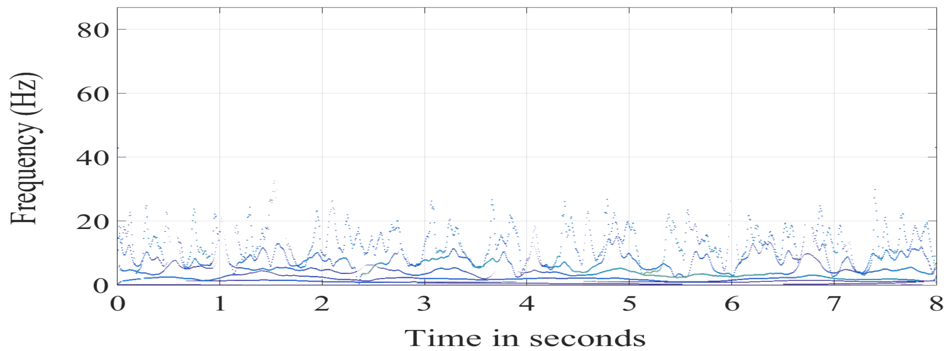

Figure 4.22: Plot of HHT based TF representation of real EEG signal.

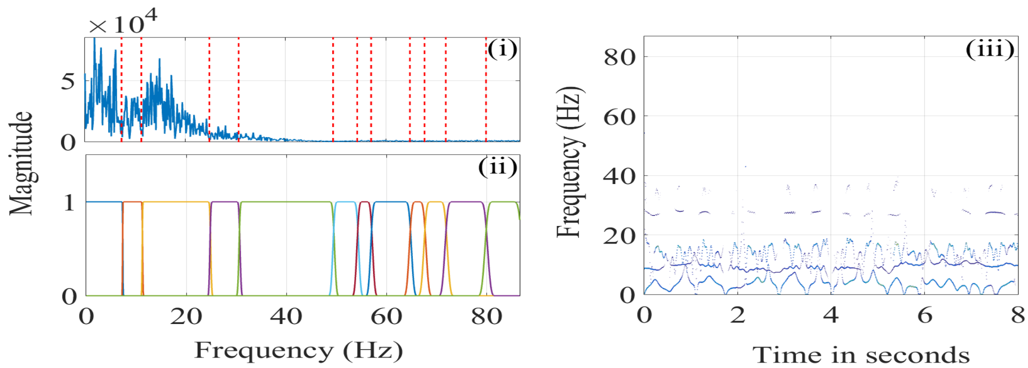

Figure 4.23: Plots of (i) the detected boundaries in the FFT spectrum, (ii) generated EWT based filter bank, and (iii) EWT based TF representation of real EEG signal.

In the previous section, we have presented the performance of the proposed FBSE-EWT based TF representation method and compared with HHT and existing EWT methods. The obtained results demonstrate that proposed FBSE-EWT provides better TF representation as compared to HHT and EWT methods especially

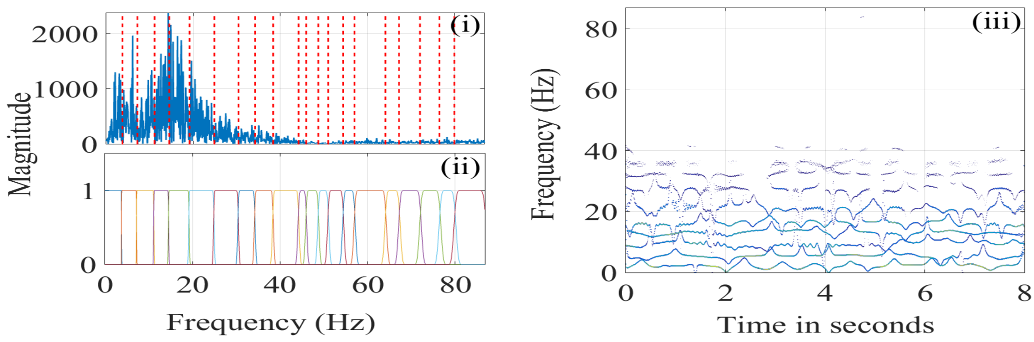

Figure 4.24: Plots of (i) the detected boundaries in the FBSE spectrum, (ii) generated FBSE-EWT based filter bank, and (iii) FBSE-EWT based TF representation of real EEG signal.

when analyzed signals have closely spaced frequency component. The existing EWT method is not successful to estimate the desired boundary frequencies when signal frequency components are very closely spaced. This is due to low frequency resolution of FFT spectrum. It also becomes very difficult to identify components in FFT spectrum when the analyzed signal is of short duration. On the other hand, FBSE spectrum has twice frequency resolution as compared to FFT spectrum. Thus, it is more advantageous to use FBSE spectrum as compared to FFT spectrum in order to estimate the optimal boundary frequencies. There exist several algorithms for the efficient computation of FBSE coefficients such as: expansion of the function into Gaussian-Laguerre (G-L) functions [85], using interpolated FFT values of the function given [75], dual algorithm based on Fourier selection summation method and Bessel function large argument asymptotic expansion [86], one-dimensional Fourier transform followed by iterated additions of preselected Fourier components [87]. These algorithms can be used for computation of FB coefficients in faster way. In the literature, there has been effort for estimating the optimal boundary frequencies in order to build wavelet based filter bank. In [60], authors replaced FFT spectrum with multiple signal classification (MUSIC) spectrum for estimating the optimal boundary frequencies [88]. However, the model order is required in advance for the MUSIC spectrum. In Figure 4.25, we have presented the MUSIC-EWT based TF

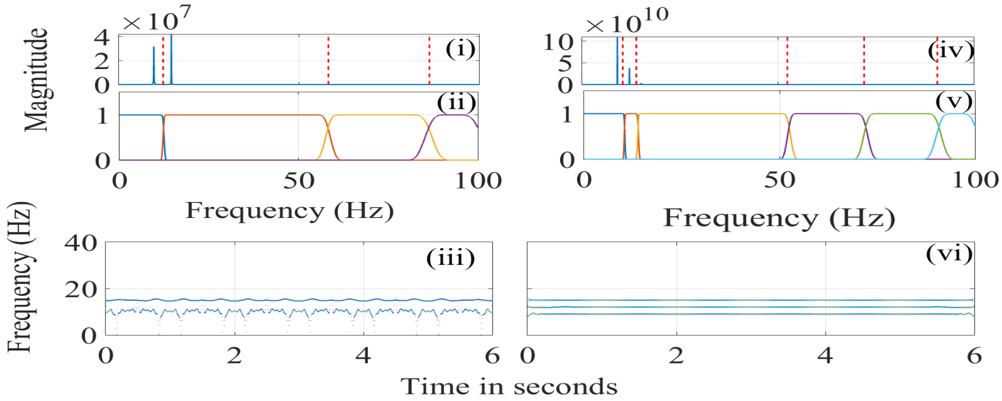

Figure 4.25: Plot of (i) the detected boundaries in the MUSIC spectrum (model order = 4), (ii) MUSIC-EWT based filter-bank, and (iii) MUSIC-EWT based TF representation for multi-component AM signal of case 3. Plot of (iv) the detected boundaries in the MUSIC spectrum (model order = 6), (v) MUSIC-EWT based filter-bank, and (vi) MUSIC-EWT based TF representation for multi-component AM signal of case 3.

representation for multi-component AM signal of case 3 (discussed in subsection 4.1) with model orders 4 and 6, respectively. The respective boundary frequencies and MUSIC-EWT based filter banks are also shown in the figure. It can be seen that MUSIC-EWT provides desired TF representation for order 6. The problem can be more severe in case of the TF representation of non-stationary signals like EEG signals where prior information of number of signal components are unknown. In Figures. 4.26 and 4.27, we have presented the MUSIC-EWT based TF representation of real EEG signal (discussed in section 4.3) for model orders 6 and 20, respectively. It can be seen that, MUSIC-EWT achieved better TF representation with model order 20. Thus, if the number of components in the signal is unknown, then a fine tuning is recommended in the MUSIC-EWT algorithm. However, our proposed method does not require any prior information about the presence of number of signal components. The method presented in this paper is suitable for the TF representation of the signals whose components do not overlap in frequency. If the signal components overlap in frequency domain, obtaining optimal boundary frequencies for segmenting the spectrum will be difficult. In future, it will be interesting to develop EWT based algorithm for representing signals whose components

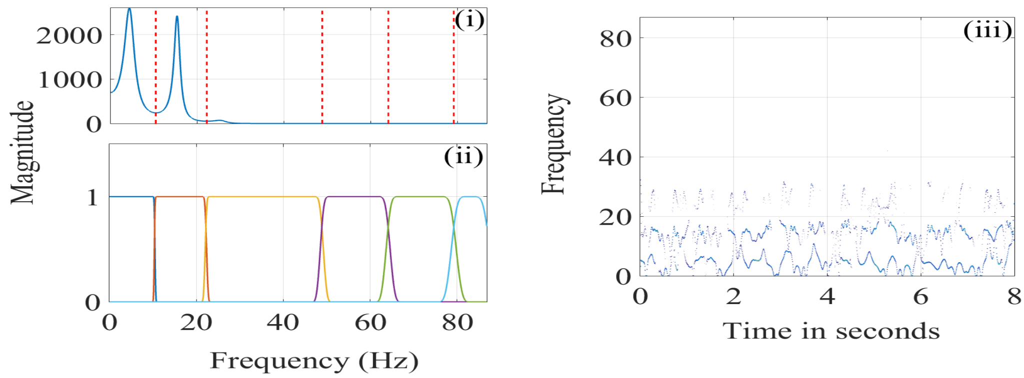

Figure 4.26: Plots of (i) the detected boundaries in the MUSIC spectrum (model order = 6), (ii) MUSIC-EWT based filter-bank, and (iii) MUSIC-EWT based TF representation of real EEG signal.

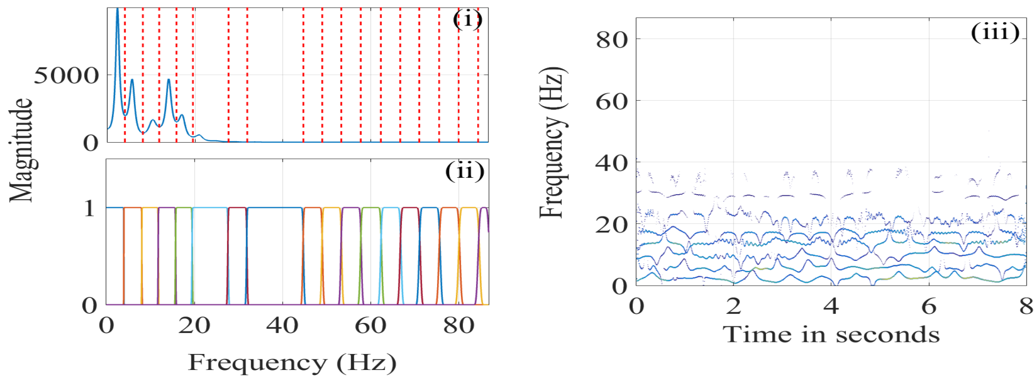

Figure 4.27: Plots of (iv) the detected boundaries in the MUSIC spectrum (model order = 20), (v) MUSIC-EWT based filter-bank, and (vi) MUSIC-EWT based TF representation of real EEG signal.

overlap in frequency domain but disjoint in TF plane.

4.4 Summary

We have taken multicomponent AM signals and multicomponent FM signals for signal analysis. For each signal, we have considered three cases. In the first case, signal components are very closely spaced. For the second and third cases, frequency spacing among the components was increased. The intention behind considering three cases is to determine whether the FBSE-EWT method can reproduce each of the signal components in the TF plane without interference. The signal duration is considered to be 6 seconds for the first case. Further, in order to observe the effect of signal duration in the detection of optimal boundary frequencies, we have increased the signal duration. In some cases, we can see that FFT based spectrum also has three components like FBSE spectrum, but the optimal boundary frequencies are detected in the FBSE spectrum only. This is due to the fact that FBSE spectrum provides better frequency resolution as compared to FFT spectrum. The performance of the TF representation has been quantitatively measured by computing MSE. The MSE value for the FBSE- EWT method is the lowest among all. After applying the scale-space based boundary detection method, six initial minima were detected. However, after length based thresholding operation, scale-space method detected only two boundary frequencies and failed to detect the other two desired boundaries. In contrast to FBSE spectrum, four boundaries were detected after thresholding operation, which included two desired boundary frequencies. This is due to the fact that FBSE spectrum has twice frequency resolution as compared to FFT spectrum.The FBSE-EWT method was also applied to the real epileptic seizure EEG signal for the TF representation. The FBSE-EWT provides more clear TF representation of the frequency component in low as well as in high region. The performance of the FBSE-EWT method has been compared with HHT and existing EWT method. The FBSE-EWT has clear advantage over EWT and HHT in the TF representation of non-stationary signals.

Chapter 5

Conclusion and future work

5.1 Conclusion

We have presented a new FBSE-EWT method for the TF representation of non-stationary signals. The FFT spectrum has been replaced with FBSE spectrum for the estimation of optimal boundary frequencies . Then scale-spaced based boundary detection method was applied, which works on the concept of two local minima, thus resulted into improved wavelet based filter bank. Ostu's method has been applied for determining the threshold value. Instead of using HT to compute IA and IF functions from the narrow band signal components, we have used NHT and based on that TF representation was generated for analysing multi-component non-stationary signals. The performance of TF representation was quantitatively measured by computing MSE of the expected TF representation and the TF representation of the considered multi-component synthetic signal. The proposed method has been applied to multi-component AM signals, multi-component FM signals, and real EEG signal for TF representation. For the AM and FM multi-component signals, we have considered three different cases and then compared FBSE-EWT with HHT, EWT, and MUSIC-EWT methods. The experimental results have shown that the proposed algorithm provides better TF representation in comparison to existing EWT method and HHT method. Thus, the proposed FBSE-EWT method has potential to analyze wide classes of real life non-stationary signals.

5.2 Future work

The presented research work can be applied on synthetic signals and real EEG signal. Further, we can explore the FBSE-EWT for the multivariate signals in order to determine the joint instantaneous amplitude and frequencies in signal adaptive frequency scale. The multivariate extension of FBSE-EWT can be developed in future. This work can also be extended to 2D signals. The proposed method can be studied for various non-stationary signals like as EEG, ECG, EMG, etc. The feature set can be obtained from the proposed FBSE-EWT method and can be studied for classification of normal and abnormal categories of various physiological signals.

Bibliography

[1] Y. Ephraim and H.L. Van Trees, "A signal subspace approach for speech enhancement," *IEEE Transaction on Speech and Signal Processing*, vol. 3(4), pp. 251-266, 1995.

[2] T.S. Kumar, M.A. Hussain, and V. Kanhangad, "Classification of voiced and non-voiced speech signals using empirical wavelet transform and multilevel local patterns," *IEEE International Conference on Digital Signal Processing(DSP)*, Singapore, pp. 163-167, 2015.

[3] S.G. Chang, B. Yu, and M. Vetterli, "Adaptive wavelet thresholding for image denoising and compression," *IEEE Transacations on Image Processing*, vol. 9(9), pp. 1532-1546, 2000.

[4] J.L. Starck, E.J. Candes, and D.L. Donoho, "The curvlet transform for image denoising," *IEEE Transactions on Image Processing*, vol. 11(6), pp. 670-684, 2002.

[5] R.B. Pachori and P. Sircar, "Speech analysis using Fourier-Bessel expansion and discrete energy separation algorithm," *In 12th Digital Signal Processing Workshop, 4th-Signal Processing Education Workshop* pp. 423-428, 2006.

[6] P. Noll, "MPEG digital audio coding," *IEEE Signal Processing Magazine*, vol. 14(5), pp. 59-81, 1997.

[7] A. Skodras and C. Christopoulos, "The JPEG 2000 still image compression standard," *IEEE Signal Processing Magazine*, vol. 18(5), pp. 36-58, 2001.

[8] G.K. Wallace, "The JPEG still picture compression standard," *IEEE Transactions in Consumer Electronics* , vol. 38(1), pp. 30-44, 1992.

[9] M. Richards, "Fundamental of radar signal processing," *McGraw-Hill Professional*, New York, NY, 2005.

[10] S. Haykin, "Adaptive radar signal processing," *Hoboken*, NJ, Wiley, 2007.

[11] G.B. Giannakis, Y. Hua, P. Stoica, and L. Tong, "Signal processing advances in wireless and mobile communications, volume 1" *Trends in Channel Estimation and Equalization*, Upper Saddle River, NJ: Prentice-Hall, 2000.

[12] R. McAulay and T. Quatieri "Speech analysis/synthesis based on a sinusoidal representation," *IEEE Transactions on Acoustics, Speech, and Signal Processing*, Vol 34(4), pp.744-754.

[13] M. Krumpholz and L.P. Katehi, "New time-domain schemes based on multiresolution analysis," *IEEE Transactions on Microwave Theory and Techniques*, Vol. 44(4), pp.555-571.

[14] K. Rolf and D. Seltzer, "Signal energy distribution in time and frequency," *IEEE Transactions on Information Theory*, Vol 14(3), pp.369-374. 1968

[15] K. Rolf and D. Seltzer, "Frequency analysis method," *U.S. Patent 5,583,784*, issued December 10, 1996.

[16] L. Cohen, "Time-frequency analysis" *Prentice hall*, Vol. 778.

[17] L. Cohen, "Time-frequency distributions a review" *Proceedings of the IEEE*, 77(7), pp. 941-981, 1989.

[18] L.B. Almeida, "The fractional Fourier transform and time-frequency representations" *IEEE Transactions on Signal Processing*, Vol. 42(11), pp. 3084-3091, 1994.

[19] H.M. Ozaktas, Z. Zalevsky, and M.A. Kutay, "The fractional Fourier Transform with applications in optics and signal processing," *New York, Wiley*, 2001.

[20] A. Bhattacharyya, R.B. Pachori, A. Upadhyay, and U.R. Acharya, "Tunable-Q wavelet transform based multiscale entropy measure for automated classification of epileptic EEG signals," *Applied Sciences*, Vol. 7(4), 385, 2017.

[21] A. Bhattacharyya, R.B. Pachori, and U.R. Acharya, "Tunable-Q wavelet transform based multivariate sub-band fuzzy entropy with application to focal EEG signal analysis," *Entropy*, Vol. 19(3), 99, 2017.

[22] R.B. Pachori, "Discrimination between ictal and seizure-free EEG signals using empirical mode decomposition," *Research Letters in Signal Processing*, Vol. 2008, 2008.

[23] S. Patidar and R.B. Pachori, "Classification of cardiac sound signals using constrained tunable-Q wavelet transform," *Expert System Application*, Vol. 41(16), pp. 7161-7170, 2014

[24] A. Bhattacharyya, M. Sharma, R.B. Pachori, P. Sircar, and U.R. Acharya, "A novel approach for automated detection of focal EEG signals using empirical wavelet transform," *Neural Computing and Applications*, Vol. 28(8), pp. 47-57, 2018.

[25] S. Lahmiri, "A variational mode decomposition approach for analysis and forecasting of economic and financial time series," *Expert System Application*, Vol. 55(C), pp. 268-273, 2016.

[26] F. Amini, N.K. Hazaveh, and A.A. Rad, "Wavelet PSO-based LQR algorithm for optimal structural control using active tuned mass dampers," *Computer Aided Civil and Infrastructure Engineering*, Vol. 28(7), pp. 542-557, 2013.

[27] M.O. Byrne, F. Schoefs, B. Ghosh, and V. Pakrashi, "Texture analysis based damage detection of ageing infrastructural elements," *Computer Aided Civil and Infrastructure Engineering*, Vol. 28(3), pp. 162-177, 2013.

[28] F. Hlawatsch and G.F. Boudreaux-Bartels, “Linear and Quadratic Time- Frequency Signal Representations,” *IEEE Signal Processing Magazine*, Vol. 9(2), pp. 21-67, 1992.

[29] M. Portnoff, “Time frequency representation of digital signals and systems based on short-time Fourier analysis” *IEEE Transactions on Acoustic Speech and Signal Processing*, Vol. 28(1), pp. 55-69, 1980.

[30] I. Daubechies, “Ten Lectures on Wavelets,” *CBMSNSF Regional Conference Series Applied Mathematics*, Philadelphia, PA, USA, 1992.

[31] B. Boashash, “Time Frequency Signal Analysis and Processing: A Comprehensive Reference,” *Academic Press*, Oxford, UK, 2003.

[32] N.E. Huang, Z. Shen, S.R. Long, M.C. Wu, H.H. Shih, Q. Zheng, N.C. Yen, C.C. Tung, and H.H. Liu, “The empirical mode decomposition and the Hilbert spectrum for nonlinear and non-stationary time series analysis,” *Proceedings of the Society of London A: Mathematical, Physical and Engineering Sciences*, Vol. 454(1971), pp. 903-995, 1998.

[33] E. Sejdic, I. Djurovic, and J. Jiang “Time-frequency feature representation using energy concentration: an overview of recent advances,” *Digital Signal Processing*, Vol. 19(1), pp. 153-183, 2009.

[34] H. Tao, J.M. Zain, M.M. Ahmed, A.N. Abdalla, and W. Jing, “A wavelet-based particle swarm optimization algorithm for digital image watermarking, ” *Integrated Computer Aided Engineering*, Vol.19(1), pp. 81-91, 2012.

[35] G. Prez, A. Conci, A.B. Moreno, and J.A. Hernandez-Tamames, “Rician noise attenuation in the wavelet packet transformed domain for brain MRI,” *Integrated Computer Aided Engineering.*, Vol. 21(2), pp. 163-175, 2014.

[36] X. Jiang and H. Adeli, “Wavelet packet autocorrelation function method for traffic flow pattern analysis,” *Computer Aided Civil Infrastructure Engineering*, Vol. 19(5), pp. 324-337, 2014.

[37] I. W. Selesnicki, "Wavelet transform with tunable Q-factor," *IEEE Transactions in Signal Processing*, Vol. 59(8), pp. 3560-3575, 2011.

[38] A. Bhattacharyya, L. Singh, and R.B. Pachori, "Identification of epileptic seizures from scalp EEG signals based on TQWT," *InInternational Conference on Machine Intelligence and Signal Processing.*, 22-24 Dec. 2017.

[39] I. Daubechies, J. Lu, and H.T. Wu, "Synchrosqueezed wavelet transforms: an empirical mode decomposition like tool," *Applied and Computational Harmonic Analysis.*, Vol. 30(2), pp. 243-261, 2011.

[40] M.Sharma, P.V. Achuth, R.B. Pachori, and V.M. Gadre "A parametrization technique to design joint time-frequency optimized discrete-time biothogonal wavelet bases," *Signal Processing*, vol. 135, pp. 107-120, 2017.

[41] K. Dragomiretskiy and D. Zosso, "Variational mode decomposition,"*IEEE Transactions on Signal Processing*, Vol. 62(3), pp. 531-544, 2014.

[42] A. Upadhyay and R.B. Pachori, "Instantaneous voiced/non-voiced detection in speech signals based on variational mode decomposition," *Journal of Franklin Institute*, Vol. 352(7), pp. 2679-2707, 2015.

[43]] A. Upadhyay and R.B. Pachori, "Speech enhancement based on mEMD-VMD method," *Electronics Letters*, Vol. 53(7), pp. 502-504, 2017. 2679-2707.

[44] N.E. Huang, Z. Wu, S.R. Long, K.C. Arnold, X. Chen, and K. Blank "On instantaneous frequency," *Advance in Adaptive Data Analysis*, Vol. 1(02), pp. 177-229, 2009.

[45] Z. Yang, L. Yang, C. Qing, and D. Huang, "A method to eliminate riding waves appear- ing in the empirical AM/FM demodulation," *Digital Signal Processing*, Vol. 18(4) pp. 488-504, 2008.

[46] P. Singh, S.D. Joshi, R.K. Patney, and K. Saha, "The Fourier decomposition method for nonlinear and non-stationary time series analysis," *Proceedings of*

the Society of London A: Mathematical, Physical and Engineering Sciences, Vol. 473(2199), 2017.

[47] G.K. Apostolidis and L. J. Hadjileontiadis, "Swarm decomposition: a novel signal analysis using swarm intelligence," *Signal Processing*, Vol. 132, pp. 40-50, 2017.

[48] R.R. Sharma and R.B. Pachori, "Time-frequency representation using IEVDHM-HT with application to classification of epileptic EEG signals," *IET Science, Measurement and Technology.*, Vol. 12(1), pp. 72-82, 2018.

[49] R.R. Sharma and R.B. Pachori, "A new method for non-stationary signal analysis using eigenvalue decomposition of the Hankel matrix and Hilbert transform," *In Fourth International Conference on Signal Processing and Integrated Networks (SPIN 2017)*, Noida, India, pp. 484-488, 2017.

[50] R.R. Sharma and R.B. Pachori, "Eigenvalue decomposition of Hankel matrix based time-frequency representation for complex signals," *Circuits Systems and Signal Processing*, 2018.

[51] R.R. Sharma and R.B. Pachori, "Baseline wander and power line interference removal from ECG signals using eigenvalue decomposition," *Biomedical Signal Processing and Control*, Vol. 45, pp.33-49.

[52] R.R. Sharma and R.B. Pachori, "Improved eigenvalue decomposition-based approach for reducing cross-terms in Wigner-Ville distribution," *Circuits, Systems, and Signal Processing*, pp.1-2, 2018.

[53] R.R. Sharma, P. Chandra, and R.B. Pachori, "Electromyogram signal analysis using eigenvalue decomposition of the Hankel matrix," *International Conference on Machine Intelligence and Signal Processing*, December 22-24, 2017, Indore, India.

[54] R.R. Sharma, M. Kumar, and R.B. Pachori, "Automated CAD identification system using time-frequency representation based on eigenvalue decomposition

of ECG signals," *International Conference on Machine Intelligence and Signal Processing*, December 22-24, 2017, Indore, India.

[55] R.B. Pachori and P. Sircar, "A new technique to reduce cross terms in the Wigner distribution," *Digital Signal Processing*, Vol. 17(2), pp. 466-474, 2007.

[56] R.B. Pachori and A. Nishad, "Cross-terms reduction in the Wigner Ville distribution using tunable-Q wavelet transform," *Signal Processing*, Vol. 120, pp.288-304, 2016.

[57] J. Gilles, "Empirical wavelet transform," *IEEE Transactions on Signal Processing*, Vol. 61(16), pp. 3999-4010, 2013.

[58] J. Gilles, G. Tran, and S. Osher, "2D empirical transforms. Wavelets, ridgelets, and curvelets revisited," *SIAM Journal on Imaging Sciences*, Vol. 7(1), pp. 157-186, 2014.

[59] A. Bhattacharyya and R.B. Pachori, "A multivariate approach for patient-specific EEG seizure detection using empirical wavelet transform," *IEEE Transactions on Biomedical Engineering*, Vol. 64(9), pp. 2003-2015, 2017.

[60] J. P. Amezquita-Sanchez and H. Adeli, "A new music-empirical wavelet transform methodology for time-frequency analysis of noisy nonlinear and non-stationary signals, " *Digital Signal Processing* Vol. 45, pp. 55-68, 2015.

[61] E.O. Brigham, "The fast Fourier transform and its applications," *prentice Hall Englewood Cliffs, NJ*, Vol. 448, 1998.

[62] K. Katoh, K. Misawa, K. Kumar, and T. Miyata, "A novel method for rapid multiple sequence alignment based on fast Fourier transform," *Nucleic Acids Research*, Vol. 30(14), pp. 3059-3066, 2002.

[63] K. Gopalan, T.R. Anderson, and E.J. Cupples, "A comparison of speaker identification results using features based on cepstrum and Fourier-Bessel ex-

pansion," *IEEE Transactions on Speech and Audio Processing*, Vol. 7(3), pp. 289–294, 1999.

[64] R.B. Pachori and P. Sircar, "Analysis of multicomponent AM-FM signals using FB-DESA method," *Digital Signal Processing*, Vol. 20(1), pp. 42-62, 2010.

[65] P. Jain and R.B. Pachori, "Time-order representation based method for epoch detection from speech signals," *Journal of Intelligent Systems*, Vol. 21(1), pp. 79-95, 2012.

[66] J. Gilles and K. Heal, "A parameterless scale-space approach to find meaningful modes in histograms- Application to image and spectrum segmentation," *International Journal of Wavelets, Multiresolution and Information Processing*, Vol. 12(06), 2014.

[67] F. Mokhtarian and B. Miroslaw, "Curvature scale space representation: theory, applications, and MPEG-7 standardization," *Springer Science and Business Media*,Vol. 25, 2003.

[68] N. Otsu, "A threshold selection method from gray-level histograms," *IEEE Transactions on Systems, Man, and Cybernetics*, Vol. 9(1), pp. 62-66, 1979.

[69] J. Schroeder, "Signal processing via Fourier-Bessel series expansion," *Digital Signal Processing*,Vol. 3(2), pp.112-124, 1993.

[70] R.B. Pachori and P. Sircar, "EEG signal analysis using FB expansion and second-order linear TVAR process," *Signal Processing*, Vol. 88(2), pp. 415-420, 2008.

[71] P. Jain and R.B. Pachori, "Event-based method for instantaneous fundamental frequency estimation from voiced speech based on eigenvalue decomposition of the Hankel matrix," *IEEE Transactions on Audio, Speech and Language Processing*, Vol. 22(10), pp. 1467–1482, 2014.

[72] R.B. Pachori and P. Sircar, "Non-stationary signal analysis: methods based on Fourier-Bessel representation," *LAP LAMBERT Academic Publishing*, Germany, 2010.

[73] C. Chen, K. Gopalan, and P. Mitra, "Speech signal analysis and synthesis via Fourier-Bessel representation," *In Acoustics, Speech, and Signal Processing, IEEE International Conference on ICASSP*, Vol. 10, pp. 497-500, 1985

[74] J. Bird and D. George "The use of the Fourier-Bessel series in calculating error probabilities for digital communication systems," *IEEE Transactions on Communications*, Vol. 29(9), pp.1357-1365, 1981.

[75] K. Gopalan and C. Chen, "Numerical evaluation of Fourier-Bessel series expansion," *IEEE International Conference on Acoustics, Speech, and Signal Processing*, ICASSP'83., Vol. 8, pp. 151–154, 1983

[76] L. Cohen and C. Lee, "Instantaneous frequency, its standard deviation and multicomponent signals," *Proceedings of SPIE*, Vol. 975, pp. l86-208, 1988.

[77] P. Maragos, J.F. Kaiser, and T.F. Quatieri, "Energy separation in signal modulations with application to speech analysis," *IEEE Transactions on Signal Processing*, Vol. 41(10), pp. 3024-3051, 1993.

[78] P. Jain and R.B. Pachori, "An iterative approach for decomposition of multicomponent non-stationary signals based on eigenvalue decomposition of the Hankel matrix," *Journal of the Franklin Institute*, Vol. 352(10), pp. 4017–4044, 2015.

[79] J.L. Semmlow and B. Griffel, "Biosignal and Medical Image Processing," *CRC Press*, 2014.

[80] R.B. Pachori and D. Hewson, "Assessment of the effects of sensory perturbations using Fourier–Bessel expansion method for postural stability analysis," *Journal of Intelligent Systems*, vol. 20(2), pp. 167-186, 2011.

[81] Z. Wang and A.C. Bovik, "Mean squared error: Love it or leave it A new look at Signal Fidelity Measures," *in IEEE Signal Processing Magazine*, vol. 26, no. 1, pp. 98-117, Jan. 2009

[82] A. S. Hood, R.B. Pachori, V.K. Reddy, and P. Sircar, "Parametric representation of speech employing multi-component AFM signal model," *International Journal of Speech Technology*, Vol. 18(3), pp. 287–303, 2015.

[83] A. Nuttall and E. Bedrosian, "On the quadrature approximation to the Hilbert transform of modulated signals," *Proceedings of the IEEE*, Vol. 54 (10), pp. 1458-1459, 1966

[84] R.G. Andrzejak, K. Lehnertz, F. Mormann, C. Rieke, P. David, and C.E. Elger, "Indications of nonlinear deterministic and finite-dimensional structures in time series of brain electrical activity: dependence on recording region and brain state,", *Physical Review*, Vol. 64(6) 2001.

[85] E. Cavanagh and B. Cook, "Numerical evaluation of Hankel transforms via Gaussian-Laguerre polynomial expansions," *IEEE Transactions on Acoustics, Speech, and Signal Processing*, Vol. 27(4), pp. 361–366, 1979.

[86] S. Candel, "Dual algorithms for fast calculation of the Fourier-Bessel transform," *IEEE Transactions on Acoustics, Speech, and Signal Processing*, Vol. 29(5), pp. 963-972, 1981.

[87] S. Candel, "An algorithm for the Fourier-Bessel transform," *Computer Physics Communications*, Vol. 23(4), pp. 343–353, 1981.

[88] T. Li and Y. Tang, "Frequency estimation based on modulation FFT and MUSIC algorithm," *First International Conference on in Pervasive Computing Signal Processing and Applications PCSPA*, pp. 525-528, 2010.